JOURNAL OF PETROLOGY | VOLUME 45 | NUMBER 3 | PAGES 609–634 | 2004 | DOI: 10.1093/petrology/egg095

Tracing Lithosphere Evolution through the Analysis of Heterogeneous G9–G10 Garnets in Peridotite Xenoliths, II: REE Chemistry

SIMON R. BURGESS* AND BEN HARTE†

GRANT INSTITUTE, SCHOOL OF GEOSCIENCES, UNIVERSITY OF EDINBURGH, KING'S BUILDINGS, EDINBURGH EH9 3JW, UK

RECEIVED FEBRUARY 14, 2000; ACCEPTED AUGUST 7, 2003

Following previous publication of major–minor element data, this paper presents rare earth element (REE) data for heterogeneous (chemically zoned) garnets belonging to the peridotite suite of mantle xenoliths from the Jagersfontein kimberlite pipe, South Africa. The rim compositions of the garnets in the highest temperature–pressure (deepest) deformed peridotites show a typical megacryst-like pattern, of very low light REE (LREE) increasing through the middle REE (MREE) to a plateau of heavy REE (HREE) at c. *20 times chondrite; these compositions would be in equilibrium with small-volume melts of the mid-ocean ridge basalt (MORB) source (asthenosphere). With decreasing depth the garnet rims show increasing LREE and decreasing HREE, eventually resulting in humped relative abundance patterns. A set of compositions is calculated for melts that would be in equilibrium with the garnet rims at different depths. These show decreasing relative abundance of each REE from La to Lu, and the La/Lu ratio of the melts increases with decreasing depth of formation. Modelling of the effects of crystal fractionation shows that this process could largely generate the sequence of garnet rim and melt compositions found with decreasing depth, including the humped REE patterns in high-level garnets. Considering the behaviour of major–minor elements as well as REE, a process of percolative fractional crystallization is advocated in which megacryst source melts percolate upwards through peridotites and undergo fractionation in conjunction with exchange with the peridotite minerals. The initial megacryst melt probably includes melt of lithospheric origin as well as melt from the MORB source, and it is suggested that the process of percolative fractional crystallization may form a variety of metasomatic and kimberlitic melts from initial megacryst melts. Repeated metasomatism of the lower lithosphere by such differentiating melts is suggested by consideration of garnet core compositions. Such metasomatism would progressively convert harzburgites to lherzolites by increasing their CaO content, and this may account for the fact that the Cr-rich diamond–garnet harzburgite paragenesis is commonly preserved only where it has been encapsulated in diamonds.*

KEY WORDS: *cratonic lithosphere; garnet zoning; mantle xenoliths; megacryst magma; metasomatic melt*

INTRODUCTION

Detailed geochemical studies of the composition of the sub-cratonic mantle lithosphere, as seen in xenoliths from kimberlites, have revealed several enigmatic features. Typical coarse peridotite xenoliths commonly show a decoupling of major and trace elements in which a depleted major element chemistry is associated with incompatible trace element enrichment (e.g. Shimizu, 1975; Harte & Hawkesworth, 1989). This has led to models in which trace element metasomatism is unaccompanied by more overt signs of metasomatism, such as changes in mineral constituents and their proportions (e.g. Harte, 1983; Dawson, 1984). Evidence of similarities in chemical composition between common megacrysts (believed to crystallize from deep-seated melts) and minerals in deformed peridotite xenoliths from kimberlite have also been demonstrated (e.g. Nixon & Boyd, 1973*a*, 1973*b*), but the detailed petrogenetic origin of this relationship has remained uncertain. Similarly, the relationship between the relatively fertile (in major elements) deformed xenolith mantle

*Present address: Oxford Instruments, Halifax Road, High Wycombe HP12 3SE, UK.
†Corresponding author. Telephone: 0131 650 8528. Fax: 0131 668 3184. E-mail: ben.harte@glg.ed.ac.uk

and the depleted (in major elements) coarse xenolith lithosphere has been a matter of debate. Some views favour a relatively primary (asthenospheric) origin for the more fertile deformed peridotites (e.g. Nixon & Boyd, 1973*a*, 1973*b*; Boyd, 1987), whereas others suggest a metasomatic origin in association with melts that also give rise to megacryst magmas (e.g. Ehrenberg, 1979, 1982; Gurney & Harte, 1980; Harte, 1983).

Evidence of the importance of metasomatic processes has continued to grow (e.g. the collection of papers in the book by Menzies & Hawkesworth, 1987; Smith & Boyd, 1987; Griffin *et al*., 1989, 1999*b*; Harte & Hawkesworth, 1989). It is now apparent that metasomatic fluids are usually melts (e.g. Eggler, 1987; Harte *et al*., 1987, 1993; Bodinier *et al*., 1990), and previous concerns over the extensive mobility of small amounts of melt in a silicate framework have been answered by considerations of surface tension and mathematical modeling of the mobility of small melt fractions (e.g. McKenzie, 1989). At the same time attention has been drawn to the importance of fluid–rock exchange reactions (often referred to as 'chromatographic effects' and possibly including mineral dissolution and precipitation) in affecting the chemical evolution of minerals and fluids during the infiltration and percolation of metasomatic fluids or melts (e.g. Navon & Stolper, 1987; Bodinier *et al*., 1990; Vernières *et al*., 1997; Ionov *et al*., 2002*a*, 2002*b*). For cratonic (kimberlite-derived) peridotites, Harte *et al*. (1993) emphasized the importance of such exchange interaction coupled with fractional crystallization in controlling the evolving metasomatic melt compositions, and referred to the combined processes as 'percolative fractional crystallization'. Similar recognition of the importance of these combined processes in alpine peridotites, xenoliths in basalts and abyssal peridotites has given rise to the essentially equivalent terms of 'reactive porous flow' (Bodinier *et al*., 1990; Bedini *et al*., 1997) and 'assimilation–reaction–fractionation' (Dick & Natland, 1996).

In seeking links between megacrysts, deformed peridotites and coarse peridotites in the mantle sample from kimberlites, Harte *et al*. (1993) used possible continuities in trace element compositions to suggest that metasomatism in the sub-cratonic mantle might be viewed as an evolutionary process. Thus it was suggested that upwelling melt (initially compositionally related to the Cr-poor megacrysts) infiltrated and metasomatized the deeper (deformed xenolith) mantle, and then percolated upwards towards shallower (coarse xenolith) mantle whilst evolving by percolative fractionational crystallization. At deeper levels, metasomatism of the peridotites involved the changing of pre-existing mineral compositions in major, minor and trace elements. At high levels mineral chemical compositions were changed mainly by trace element enrichment in incompatible elements, although new phases (e.g. phlogopite, amphibole) might be precipitated as a result of increasing concentrations of elements such as K and Na. The proposals of Harte *et al*. (1993) were based on very limited trace element data from a number of southern African localities, so that progressive evolution at one locality could only be inferred. Bedini *et al*. (1997) and Ionov *et al*. (2002*a*) used a plate model of porous reactive flow to suggest genetic connections between different sets of xenoliths. In all cases the links of chemical evolution between xenoliths were largely inferred and there was little evidence of progressive evolution within individual xenoliths.

Burgess (1997) and Burgess & Harte (1999) have now studied garnet compositions in 50 peridotite samples from one kimberlite pipe. This is the Jagersfontein pipe of type 1 kimberlite, which erupted through the Kaapvaal craton (South Africa) at 83 Ma (Smith, 1983). From detailed major and minor element data, Burgess & Harte (1999) provided evidence for upward percolation of a melt with an initial melt composition related to that of the melt that crystallized Cr-poor megacrysts. In addition, the presence of preserved heterogeneities in garnet in about half of the samples studied allowed Burgess & Harte (1999) to show the importance of both mineral growth (causing crystal fractionation) and melt–matrix exchange as driving forces for melt evolution, as expected in a percolative fractional crystallization process.

This paper represents the continuation of this integrated grain- and xenolith-scale study of garnets from the Jagersfontein peridotite suite, and examines the evidence provided by rare earth element (REE) data on the geochemical evolution of the sub-cratonic mantle sampled at Jagersfontein. The evidence is particularly focused on the nature of the initial melt and its compositional evolution during the metasomatic (infiltration–reaction) process, but the potential relations of the percolating and fractionating melt to other mantle metasomatic fluids or melts are also considered. In addition, the evolution of lower-lithosphere peridotites and the manner of formation of humped garnet REE patterns in lherzolites and harzburgites is discussed. There is important evidence for the conversion of garnets of G10 (Ca-poor) harzburgite paragenesis (e.g. Sobolev, 1977; Gurney, 1984) to G9 lherzolite paragenesis, which we believe has a bearing on the distribution of the diamond–garnet harzburgite paragenesis frequently identified in diamond exploration and mining. Furthermore, we believe that the repetition of metasomatic events in the mantle lithosphere provides an important basis for understanding the multi-faceted and enigmatic geochemical features referred to above.

ANALYTICAL TECHNIQUES

Trace element analysis was carried out by the secondary ion mass spectrometry (SIMS) technique using the Cameca ims 4f ion probe at the University of Edinburgh. Samples were analysed during two analysis sessions in September 1994 and January 1996. Analytical conditions are summarized in Table 1. The analytical procedures broadly followed those described by Zinner & Crozaz (1986). A $^{16}O^-$ primary ion beam from a duo-plasmatron source was used, with a primary mass analyser to filter out other molecular species. The primary accelerating voltage was 10 kV, and the beam was focused with electrostatic lenses to a 20–40 μm spot on the polished surface of a 1 inch round sample section. To reduce molecular interferences in the secondary ion mass spectrum, a 75 V high-energy offset was used and secondary ions were separated by mass/charge ratio in the mass analyser, with the measurements of the different ions quantified by repetitive cycling through the mass peaks in an automatic peak jumping mode. The dwell time on each mass peak was typically 5 s. Each analysis was made up of 8–10 cycles through the mass spectrum, and therefore total count times on mass peaks were usually 40–50 s. The ions were detected by an electron multiplier, and the ion counts determined for each mass peak were corrected to account for the background count rate and dead time of the electron multiplier and counting system.

Elemental concentrations were calculated using relative ion yields (RIYs) for the elements, which were determined from measurements on standards of known concentration. The principal standard used was the silicate glass SRM610, in which a nominal 500 ppm of the trace elements was assumed (Hinton, 1990). Ion yields were calculated for each element relative to a reference element, in this case silicon. The SRM610 standard was analysed at least three times during each analysis day, and its relative ion yields were periodically checked against those of standard garnet and clinopyroxene minerals. For the garnet analyses reported here, there was no evidence for the need of a matrix correction between garnet and the SRM610 glass standard. The RIYs used for each unknown were averages of those calculated for the standard readings taken prior and subsequent to the analysis of the unknown. By this method, changes in RIY with time were taken into account. The contribution of oxide interferences from each mass peak was removed by subtraction. The analysis of oxide and element peaks in high trace element concentration glasses (e.g. calcium aluminium silicate and apatite glasses) has shown that element/oxide ratios are not sensitive to matrix composition. Therefore, by determining one element/oxide ratio in an unknown (typically Nd/NdO) all the other REE/REEO ratios can be determined and the oxides subtracted from the intensities of the different masses. Further details of the analytical procedure, errors and data reduction have been reported by Burgess (1997) and Harte & Kirkley (1997). Representative REE analyses of garnet cores and rims are given in Table 2. The complete dataset for the Jagersfontein xenoliths forming part of this study is given in the Burgess (1997) Ph.D. thesis, copies of which are lodged at the Universities of Edinburgh and Cape Town and at the De Beers Geoscience Centre, Johannesburg. The dataset can be downloaded from the *Journal of Petrology* web site at http://www.oupjournals.org.

Table 1: Ion microprobe operating conditions

	September 1994	January 1996
Primary beam polarity	negative	negative
Primary ion beam	O^-	O^-
Accelerating voltage	10 kV	10 kV
Beam current	8 nA	15 nA
Secondary beam polarity	positive	positive
Offset	~78 V	~78 V
Energy window	±19 eV	±19 eV
Number of cycles	10	8
Count time per cycle	5 s for most elements (10 s for Nb, Ce, Nd, Sm, Eu)	5 s for all elements
Deadtime	32 ns	14 ns

SELECTION OF PARTITION COEFFICIENTS

Direct determination of partition coefficients between crystals and melt requires detailed high-temperature experiments, but these are often bedevilled by experimental problems of achieving equilibrium and minimizing quench effects, together with difficulties of quantifying compositions in fine-grained experimental charges. For deep lithospheric mantle situations, as considered here, the major silicate minerals carrying trace elements are clinopyroxene and garnet, and for these minerals the same experiment results are used in many papers, including those carrying compilations of partition. Unfortunately, commonly used sets of partition coefficients (e.g. Grutzeck *et al.*, 1974; Shimizu & Kushiro, 1975; McKenzie & O'Nions, 1991) do not yield consistent results if applied to the determination

Table 2: Representative ion microprobe analyses of REE in garnet cores and rims

Sample:	JJG1728 core	JJG1728 rim	J146 core	J146 rim	J22 core	J22 rim	J107 core	J107 rim	JJH19 core	JJH19 rim	J112 core	J112 rim	JJH37E core	JJH37E rim
La	0·85	0·04	0·07	0·11	0·04	0·03	0·04	0·04	0·03	0·03	0·05	0·05	0·04	0·03
Ce	5·73	0·75	0·71	0·81	0·42	0·28	0·44	0·33	0·39	0·36	0·43	0·47	0·3	0·21
Pr	0·84	0·36	0·26	0·30	0·17	0·13			0·16	0·13	0·18	0·16	0·11	0·10
Nd	4·42	3·56	2·82	3·05	2·01	1·19	1·91	1·45	1·98	1·55	1·87	1·89	0·83	0·92
Sm	1·02	1·89	1·81	1·77	0·87	0·96	1·57	1·31	1·04	1·06	1·52	1·57	0·3	0·67
Eu	0·29	0·78	0·68	0·75	0·32	0·46	0·62	0·63	0·38	0·48	0·68	0·75	0·07	0·33
Gd	0·75	2·46	1·78	2·55	0·96	1·68	2·76	2·72	0·99	1·63	2·75	2·89	0·24	1·16
Tb	0·09	0·43	0·19	0·38	0·16	0·38	0·50	0·54	0·14	0·37	0·52	0·63	0·05	0·25
Dy	0·43	2·10	0·74	2·19	0·75	2·90	2·96	3·95	0·83	2·63	2·93	3·85	0·55	1·69
Ho	0·05	0·28	0·12	0·36	0·11	0·61	0·56	0·84	0·11	0·49	0·44	0·64	0·13	0·34
Er	0·12	0·41	0·36	0·82	0·34	2·15	1·61	2·38	0·24	1·29	0·91	1·42	0·59	0·97
Yb	0·13	0·28	0·60	0·96	0·43	1·99	1·57	2·44	0·29	1·23	1·01	1·12	0·93	1·29
Lu	0·03	0·04	0·12	0·16	0·06	0·30	0·26	0·41	0·06	0·19	0·17	0·19	0·17	0·93

Sample:	J110 core	J110 rim	J34 core	J34 rim	J121 core	J121 rim	J115 core	J115 rim	J75(meg) core	J75(meg) rim	J75(meg) average
La	0·03	0·03	0·03	0·03	0·03	0·04	0·03	0·03	0·03	0·02	0·02
Ce	0·37	0·29	0·24	0·22	0·28	0·29	0·17	0·22	0·18	0·19	0·18
Pr	0·15	0·10			0·09	0·10	0·07	0·07	0·06	0·07	0·07
Nd	1·46	1·22	0·94	0·94	0·95	0·98	0·72	0·70	0·82	0·80	0·81
Sm	0·88	1·02	0·76	0·74	0·57	0·61	0·57	0·65	0·70	0·72	0·71
Eu	0·44	0·49	0·38	0·34	0·24	0·28	0·24	0·36	0·35	0·37	0·36
Gd	1·53	2·06	1·67	1·62	0·98	1·12	1·00	1·32	1·75	1·77	1·76
Tb	0·34	0·49	0·4	0·31	0·24	0·26	0·25	0·32	0·44	0·45	0·44
Dy	2·53	3·78	2·81	2·72	1·81	2·02	2·03	2·35	3·82	3·76	3·79
Ho	0·53	0·87	0·67	0·60	0·42	0·46	0·48	0·59	0·89	0·95	0·92
Er	1·60	2·67	2·5	2·07	1·37	1·53	1·72	1·75	3·06	3·09	3·07
Yb	1·88	2·72	2·16	2·43	1·57	1·76	2·05	2·29	3·30	3·59	3·45
Lu	0·27	0·37	0·37	0·38	0·25	0·28	0·33	0·34	0·51	0·53	0·52

of melt compositions from natural clinopyroxene and garnet that appear to have crystallized together (e.g. Harte *et al*., 1993; Tainton & McKenzie, 1994). The clinopyroxene–melt partition coefficients of Grutzeck *et al*. (1974) are supported by the experimental work of Hart & Dunn (1993). However, these clinopyroxene–melt partition coefficients were determined at atmospheric pressure, and the extent to which they will apply to the high-pressure assemblages of mantle xenoliths and the deep mantle lithosphere is uncertain. Blundy *et al*. (1998) have shown that at moderate pressures (where garnet is generally absent in peridotites), the stabilization of an aluminous clinopyroxene results in a marked shift in partition coefficients with relatively greater uptake of middle REE (MREE) and heavy REE (HREE) by clinopyroxene. However, application of these aluminous clinopyroxene partition coefficients to deep mantle lithosphere conditions, where garnet is stable, does not appear appropriate, because the clinopyroxene compositions coexisting with garnet are similar to those of low-pressure assemblages in being relatively low in Al_2O_3.

As an alternative to experimental data, natural assemblages of minerals formed in equilibrium with one another provide an extensive source of information on inter-mineral partition coefficients and provide an important source of information on crystal chemical parameters affecting partition (e.g. Shimizu, 1975; Blundy & Wood, 1991; Harte *et al*., 1996; Harte & Kirkley, 1997). Harte *et al*. (1996) looked at the

Table 3: Mineral–melt partition coefficients for REE

	La	Ce	Nd	Sm	Eu	Gd	Dy	Er	Yb	Lu
Olivine/melt		0·0005	0·001	0·0013	0·0016	0·0015	0·0017	0·0015	0·0015	
Opx/melt		0·003	0·0068	0·01	0·013	0·016	0·022	0·03	0·049	
Cpx/melt	0·061	0·092	0·199	0·276	0·31	0·3	0·386	0·344	0·43	0·357
Garnet/melt										
$T = 1400°C$	0·0016	0·011	0·06	0·239	0·378		1·682	2·802		18·682
$T = 1300°C$	0·0011	0·008	0·049	0·21	0·345		1·592	2·702		19·203
$T = 1200°C$	0·0007	0·005	0·038	0·181	0·311		1·495	2·592		19·813
$T = 1100°C$	0·0005	0·003	0·029	0·152	0·277		1·391	2·472		20·535
$T = 1000°C$	0·0003	0·002	0·021	0·125	0·242		1·28	2·34		21·404
$T = 900°C$	0·0002	0·001	0·017	0·099	0·206		1·162	2·194		22·269

The partition coefficients for olivine/melt and orthopyroxene/melt are taken from Hanson (1980). Clinopyroxene/melt partition coefficients are the average of the data of Grutzeck *et al.* (1974) and Hart & Dunn (1993). Garnet/melt partition coefficients use clinopyroxene/garnet partition coefficents based largely on natural rock mineral data (Harte *et al.*, 1996), in conjunction with the clinopyroxene/melt data given. (See text.)

variability of clinopyroxene–garnet partition coefficients, taking care to use data for restricted peridotitic compositions and thereby avoid the problems of varying bulk [particularly Ca/(Ca + Mg + Fe)] composition effects (Harte & Kirkley, 1997; van Westrenen *et al.*, 1999). They found a consistent set of data with evidence of a linear correlation between the natural logarithm (ln D) of the garnet–clinopyroxene partition coefficients and temperature (1000/T) in the temperature range 750–1400°C. For clinopyroxene–garnet–melt partition coefficients, Harte *et al.* (1996) recommended the use of these natural clinopyroxene–garnet data in conjunction with an average of experimental clinopyroxene–melt data for low-alumina clinopyroxene (Grutzeck *et al.*, 1974; Hart & Dunn, 1993) to calculate garnet–melt partition coefficients, because the experimental garnet–melt data of Shimizu & Kushiro (1975) appear to underestimate partition coefficients for the light REE (LREE). Use of the Harte *et al.* (1996) procedure reduces the aforementioned problem of inconsistent garnet–melt and clinopyroxene–melt partition coefficients, and also provides a better fit to calculated melt compositions predicted by Tainton & McKenzie (1994) (see discussion below on megacryst melts).

Therefore, the garnet–melt partition coefficients adopted here have been determined following the Harte *et al.* (1996) procedure and have been calculated over a temperature range of 900–1400°C using the temperature dependence shown by the natural clinopyroxene–garnet partition coefficients. Any temperature dependence of the clinopyroxene–melt partition coefficients is ignored, as the experimental data of Grutzeck *et al.* (1974) and Hart & Dunn (1993) are for a very limited temperature range. The resultant garnet–melt data are given in Table 3, together with the mineral–melt partition coefficients used for other minerals as taken directly from the literature.

SUMMARY OF THE PETROLOGY OF THE JAGERSFONTEIN PERIDOTITE XENOLITH SUITE

Samples for this study were selected from extensive collections housed at the Universities of Cape Town and Edinburgh and made principally by J. J. Gurney, B. Harte, J. J. Hops and P. A. Winterburn (see Winterburn, 1987; Hops, 1989). Winterburn *et al.* (1990) used both petrography and T–P relationships to divide the xenoliths into three groups, designated low-, medium- and high-temperature suites. The xenoliths making up both the low- and medium-temperature suites are coarse, whereas the high-temperature xenoliths are deformed [terminology after Harte (1977, 1983)]. The coarse low-temperature suite is dominated by lherzolites and garnet lherzolites, the medium-temperature suite by garnet harzburgites. Some coarse xenoliths have been modally metasomatized (Field *et al.*, 1989; Winterburn *et al.*, 1990), giving rise to low-temperature xenoliths with amphibole and medium-temperature xenoliths with phlogopite and spinel (Fig. 1). In the deformed xenoliths modal metasomatic minerals are absent, but garnet and clinopyroxene are generally present in greater abundance than in coarse xenoliths (Hops *et al.*, 1989). In detail, Burgess (1997) showed that deformed peridotite xenoliths with relatively shallow depths of origin are

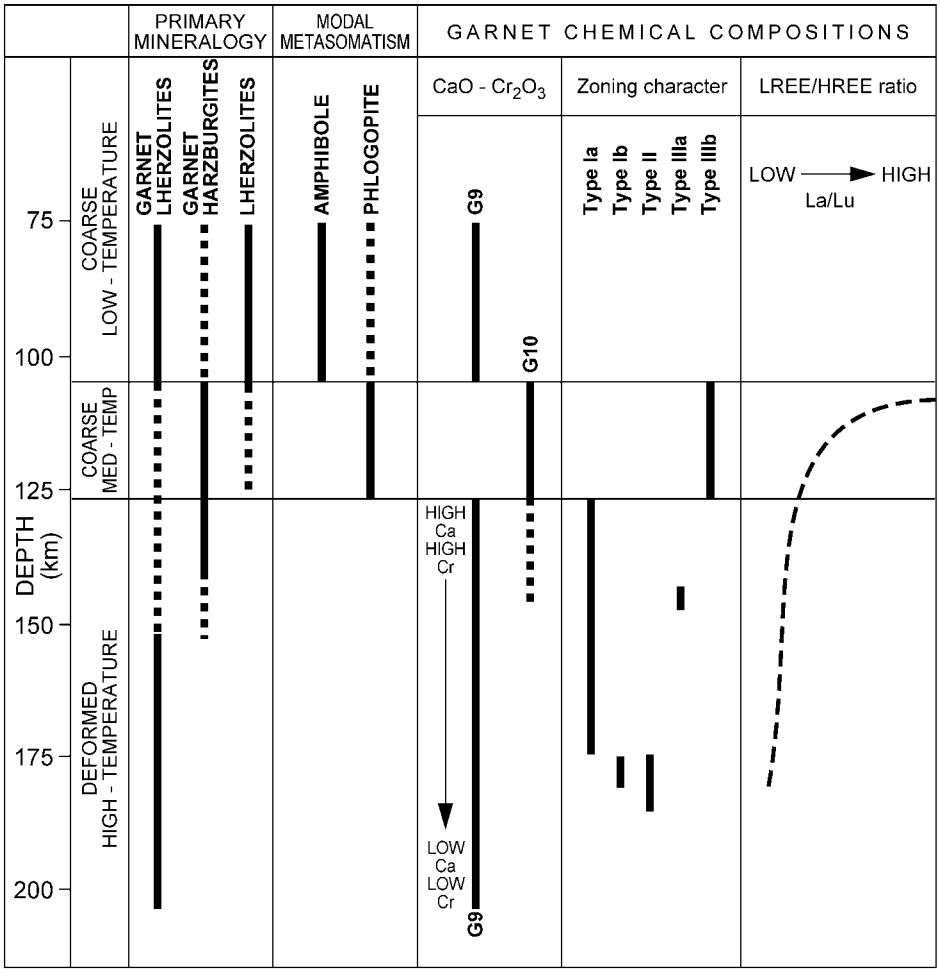

Fig. 1. Summary diagram for Jagersfontein peridotite xenoliths. The first two columns show variation with depth of peridotite primary mineralogy and modal metasomatic minerals. The remaining columns summarize aspects of the depth-related variations in garnet chemical composition including variation in the types of garnet zoning or heterogeneity [Types Ia, Ib, etc. are explained in the text and by Burgess & Harte (1999)]. The pressure–temperature data giving the depth estimates have been given by Burgess & Harte (1999).

dominantly garnet harzburgites, but that garnet lherzolites increase in abundance with depth and the deepest samples are exclusively lherzolites (Fig. 1).

Summary of garnet chemistry in the Jagersfontein peridotites and megacrysts

The major element chemistry of garnets in the peridotite xenoliths shows important trends in geochemical behaviour between and within the xenolith suites [as presented in detail by Burgess (1997) and Burgess & Harte (1999)]. The main features of garnet chemical variations are summarized in Fig. 1 and on a CaO–Cr_2O_3 plot in Fig. 2. Garnets from the coarse low-temperature suite are G9 (lherzolitic) in composition [nomenclature of Dawson & Stephens (1976) and Gurney (1984)] and plot in a small region near the base of the lherzolite trend line. In contrast, garnets from the harzburgitic coarse medium-temperature suite are G10 low-Ca garnets, and plot to the low-Ca (harzburgitic) side of the lherzolite trend. The deformed high-temperature peridotite garnets possess a wide range of G9 compositions, which largely follow the trend of the lherzolite line at Jagersfontein (Fig. 2). As emphasized by Burgess & Harte (1999), with increasing depth the CaO and Cr_2O_3 content of garnets in deformed xenoliths decreases and approaches the composition of Cr-poor megacryst garnets, which plot near the base of the lherzolite trend.

Peridotitic garnets from Jagersfontein with heterogeneous chemical compositions, shown by concentric zoning and more complex patterns of chemical variation, have been identified by Hops *et al.* (1989), Smith & Boyd (1992), Shimizu *et al.* (1994), Burgess (1997) and Burgess & Harte (1999). These chemically heterogeneous garnets are present in a significant proportion

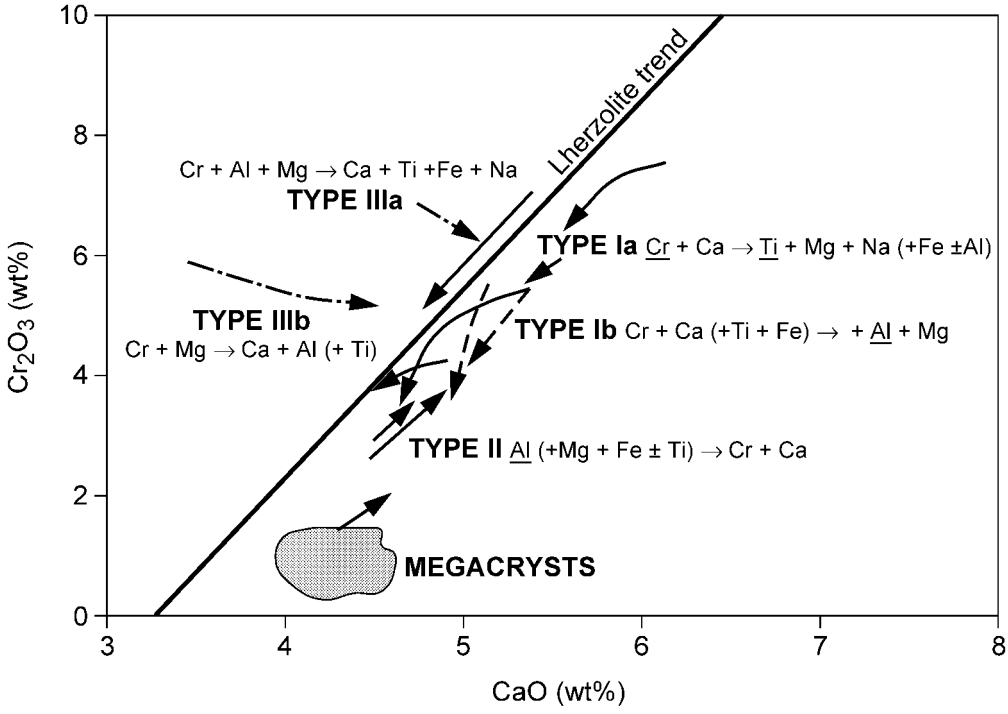

Fig. 2. Garnets of the Jagersfontein peridotite suite plotted in the CaO–Cr_2O_3 diagram. The arrowed lines show examples of the core-to-rim trends in composition of zoned garnets of Types Ia, Ib, II, IIIa and IIIb. Type Ia garnets are indicated by downward-pointing continuous-line arrows; Type Ib garnets by downward-pointing dashed-line arrows; Type II garnets by upward-pointing continuous-line arrows; Type III garnets by dot–dash-line arrows. The changes in cation composition for each zoning type are indicated in the light typeface. The range of composition of Jagersfontein megacryst garnets [data from Hops (1989)] is shown by the shaded field. Peridotite data are from Burgess (1997). Modified from Burgess & Harte (1999).

of the xenoliths from the deformed xenolith suite and have also been identified in a few samples from the coarse medium-temperature suite. However, they are entirely absent in samples from the coarse low-temperature suite. Heterogeneous garnets that are G9 in composition show chemical variations along the lherzolite trend, whereas those that are G10 show increasing CaO towards the lherzolite trend. Burgess & Harte (1999) classified the heterogeneous garnets into three main types on the basis of core–rim variation in Ca and Cr levels, as summarized below and illustrated in Fig. 2:

Type I is defined by core-to-rim decreases in Ca and Cr, along the lherzolite trend;
Type II shows core-to-rim increases in Ca and Cr, along the lherzolite trend;
Type III shows core-to-rim Ca increase and slight Cr decrease, towards the lherzolite trend.

This classification has been further subdivided for Type I and Type III variations in terms of changes in the levels of the minor element Ti. Therefore, Type Ia chemical variation is defined by core-to-rim increases in Ti, whereas in Type Ib Ti decreases from core to rim. Similarly, Type IIIa variation is defined by Ti addition from core to rim, whereas in Type IIIb Ti levels are negligible and are either constant or increase very slightly from core to rim.

Although not all deformed and coarse medium-temperature peridotite xenoliths show garnets with compositional heterogeneity, it is notable that where garnets show chemical change, then it can be clearly related to depth of origin of the xenolith (Burgess & Harte, 1999), as summarized in Fig. 1. The deformed xenolith suite is dominated by Type Ia variation. However, at relatively high pressures, towards the base of the mantle section represented by deformed xenoliths, Type Ia variation grades into Type Ib and then into Type II chemical variation. In some xenoliths garnets showing both Type Ia and Type II chemical variation occur. Type IIIa variation is shown by only one sample, a deformed harzburgite (sample JJH19), which formed at the low-pressure end of the depth range shown by xenoliths from the deformed high-temperature suite. Other deformed samples from similar depths have garnets that show indistinct substitutions. Type IIIb substitution is shown by coarse medium-temperature samples and is characterized by G10 cores that approach G9 composition on grain

rims. The specific trend shown for IIIb in Fig. 2 is that of specimen JJG1728, for which trace element data are also depicted below, but similar features have been shown by Smith & Boyd (1992), Boyd *et al.* (1993) and Griffin *et al.* (1999*b*).

The geometric arrangement, as well as the chemical nature of compositional variation within garnet grains, shows some dependence on temperature–pressure or depth (Burgess, 1997; Burgess & Harte, 1999). The most common expression of variation is concentric

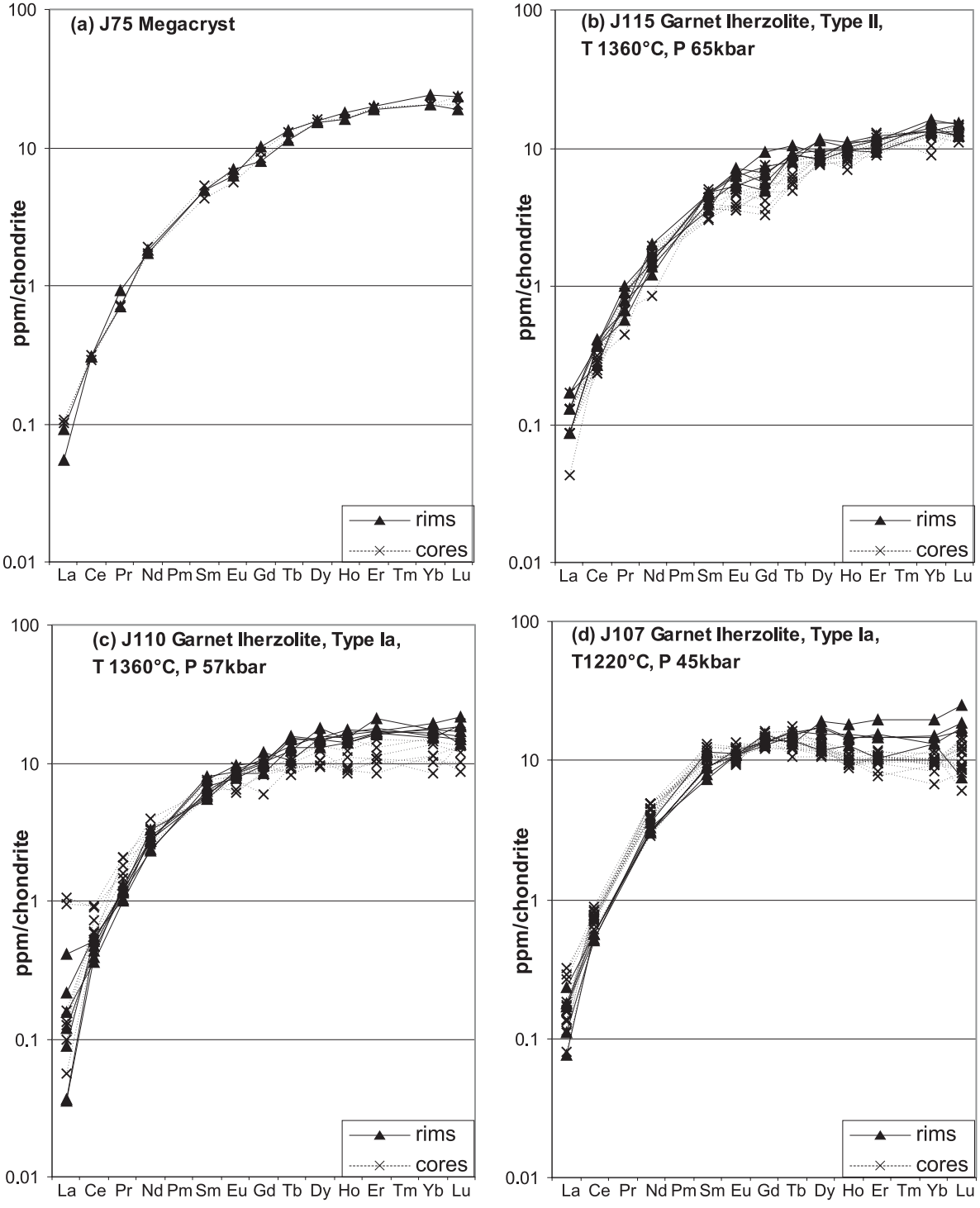

zoning with a progressive change from the core through a series of rim compositions. The shapes of the core-to-rim composition profiles show that new garnet has formed as rim overgrowths, although there is also evidence of modification of the profiles by diffusion (Griffin *et al*., 1989, 1999*b*; Burgess & Harte, 1999; Shimizu, 1999). In addition to concentric features, deformed garnets showing Type Ia substitution also commonly show cross-cutting zones, which have been identified by Matthews *et al*. (1992) as the result of hydrofracturing in the presence of infiltrating melt followed by new garnet growth from the melt. The deepest samples (i.e. those with garnets showing Type Ib and II substitution) do not commonly exhibit cross-cutting features. Type II garnets show distinctive concentric patterns in that the main core-to-rim variation of increasing Ca and Cr is reversed in a narrow zone near the rims of garnet grains. This is described as ring geometry, and it is suggested that such garnets initially underwent resorption caused by partial melting before undergoing growth forming a narrow rim at a later stage (Burgess & Harte, 1999).

TRACE ELEMENT COMPOSITIONS OF JAGERSFONTEIN GARNETS

Core and rim trace element compositions have been determined for garnets from all three peridotitic xenolith suites, ranging from high to low temperature. For the coarse medium-temperature and deformed high-temperature suites, the garnets analysed were dominantly those that are heterogeneous in terms of major elements, although homogeneous garnets were also analysed (Burgess & Harte, 1999). In the present paper we concentrate on the compositions of the heterogeneous–zoned garnets summarized above. Figure 3 shows REE plots of core and rim compositions for representative garnets from the deformed high-temperature and medium-temperature suites (see also Table 2). Data on garnets from the coarse low-temperature suite, which includes amphibole-bearing types, are omitted from this paper, as they show no compositional heterogeneity that may be compared with that of specimens of deeper origin. However, megacryst garnet compositions are considered, as they

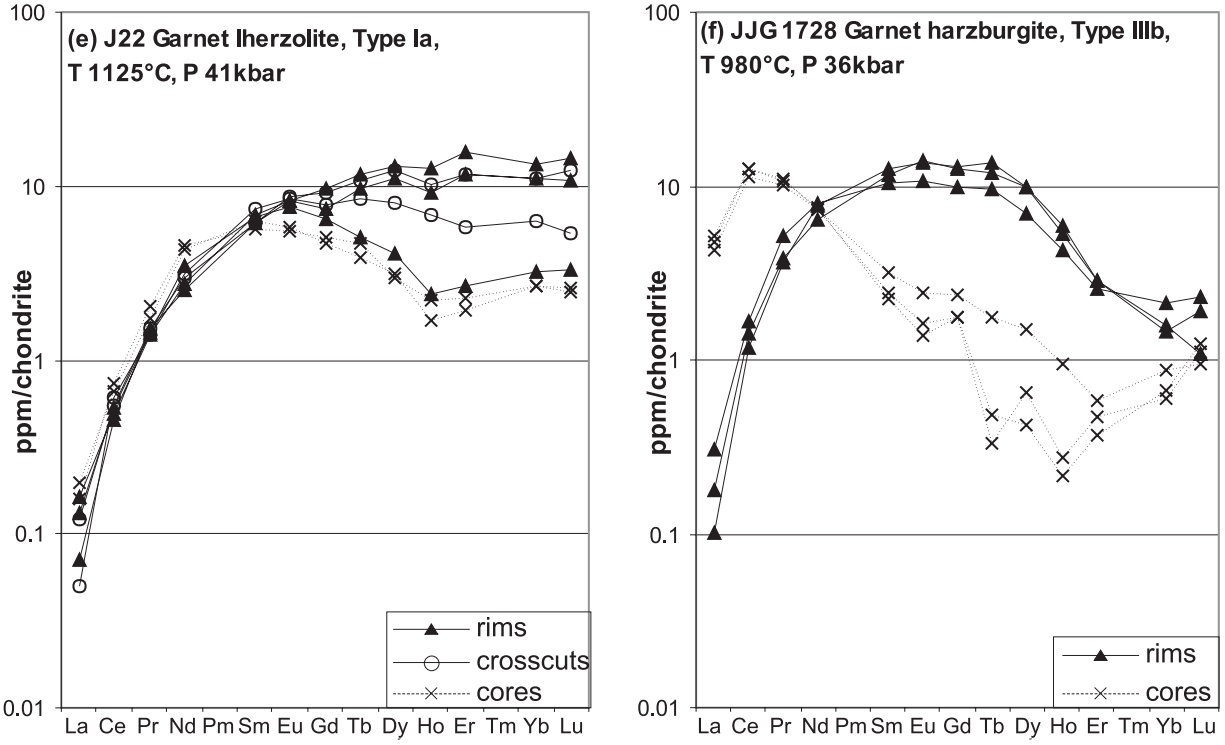

Fig. 3. REE compositions of megacryst (J75) and peridotitic garnets (J115, J110, J107, J22, JJG1728), normalized to chondritic values of Sun & McDonough (1989). The peridotitic garnets show REE compositional zoning from cores (×) to rims (▲), which complements zoning in major and minor elements. In the case of J22 there are also regions of variable composition that crosscut (○) the core [see Burgess & Harte (1999) for further discussion of zoning types and patterns]. All peridotites are deformed, except JJG1728 (which is coarse, medium-temperature peridotite). Zoning types and T–P conditions of formation of garnet rims are summarized in each diagram. Temperature–pressure estimation from Burgess (1997) following the methods of: Brey & Kohler (1990) for orthopyroxene–clinopyroxene solvus temperatures in lherzolites, and Al-in-orthopyroxene pressures; O'Neill & Wood (1979) for olivine–garnet Fe–Mg temperatures in harzburgites.

provide a marker for initial melt compositions (Burgess & Harte, 1999).

Garnets from the Cr-poor garnet megacrysts

Garnets from the Cr-poor megacryst suite (e.g. J75; Fig. 3) are characterized by an HREE-enriched plateau at 10–20 times chondrite, with LREE and MREE rising smoothly to the plateau from near 0·1 times chondrite for La. It should be noted that although described as an HREE-enriched plateau pattern, because HREE chondrite-normalized compositions are similar, there is a characteristic slight rise in the HREE compositions as one approaches Lu. This is a typical profile and composition for many Cr-poor garnet megacrysts from kimberlites (e.g. Frey, 1984), and it is also similar to that seen in many high-pressure–temperature deformed xenoliths with homogeneous garnets (e.g. Shimizu, 1975).

Garnets from the deformed high-temperature suite

Garnets that show Type Ia (G9), Type Ib (G9), Type II (G9) and Type IIIa (G10–G9) substitutions (Burgess & Harte, 1999), in addition to garnets from homogeneous samples, all occur within the high-temperature deformed suite. The dominant REE pattern shown by garnets from this suite, particularly by garnet rims, is an HREE-enriched plateau pattern (Fig. 3b–d). It is characterized by La near 0·1 times chondrite, with concentrations rising through the LREE and MREE to reach a plateau in the HREE near 10 times chondrite. Thus there are similarities between these garnet rims and the megacryst compositions, although in detail there are significant differences between the garnets analysed, as explained below. At shallower depths, in the uppermost deformed peridotites (and also in the coarse medium-temperature peridotites), the REEpatterns (Fig. 3e and f) show markedly distinct differences from the megacryst pattern and show humped profiles.

G9 garnets showing Type Ib–II major element variation

These high-pressure samples (Fig. 1), which plot towards the base of the lherzolite trend in Fig. 2, are characterized by relatively indistinct REE core-to-rim variations in garnets, usually consisting of minor increases in HREE. All patterns (both core and rim) are characterized by HREE-enriched plateaux (e.g. J115, Fig. 3b), which are closely similar in shape to the megacryst patterns, although there are small variations in the levels of abundance of the elements.

G9 garnets showing Type Ia major element variation

Type Ia major–minor chemical variation dominates garnets from the deformed xenolith suite at Jagersfontein and is therefore seen throughout a major part (130–180 km) of the mantle section (Burgess & Harte, 1999; Fig. 1). Garnets of this type (e.g. J110, Fig. 3c) show rim compositions that are mainly similar to megacrysts, and core-to-rim REE changes are dominated by increases in the level of the HREE plateau, coupled with minor decreases in LREE. However, as pressure decreases, core compositions show a progression toward humped patterns in which some MREE have greater abundance (relative to chondrite) than HREE, whereas rim compositions vary between this humped pattern and profiles that have fairly constant MREE and HREE chondrite-normalized compositions (e.g. J107, J22, Fig. 3d and e). It should be noted that these MREE–HREE patterns are distinctly flatter than those of megacrysts and type II garnets.

Garnets from the coarse medium-temperature suite

Three coarse, medium-temperature, peridotite samples have garnets that show variations in composition. Only two of these show major element heterogeneities: one (JJG1728) shows the distinctive Type IIIb (G10–G9) variation illustrated in Fig. 2, whereas the other (J146) has a much smaller range and less distinct trend of variation (Burgess & Harte, 1999). The REE compositional variations are similar in all these samples and are illustrated by core and rim compositions for JJG1728 in Fig. 3f. They are characterized by marked humps (maxima) between Ce and Dy at levels between 10 and 20 times chondrite. Comparing rims with cores, the MREE hump or maximum is closer to the HREE in the rims than the cores and the LREE/HREE ratio is lower in the rims.

TRACE ELEMENT COMPOSITION OF METASOMATIC MELTS

The evidence presented by Burgess (1997) and Burgess & Harte (1999) on the major and minor element compositions of the Jagersfontein garnets supports the findings of previous studies (e.g. Smith & Ehrenberg, 1984; Harte *et al*. 1987; Smith & Boyd, 1987; Griffin *et al*., 1989, 1999*b*; Matthews *et al*., 1992) that major element zoning in peridotitic garnets is the result of chemical modification (including garnet growth as well as diffusion) caused by interaction with a metasomatic melt. Given this, the REE compositions of garnet rims formed from the metasomatic melts are a monitor

of the compositions of the melts, and garnet–melt partition coefficients may be used to derive the compositions of the melts themselves (e.g. Harte, 1983; Harte *et al.*, 1993). In this way the composition of the rims of the heterogeneous garnets, in combination with the intersample relationships suggested by Burgess & Harte (1999), and summarized here, may be used to make inferences on the chemical evolution of metasomatic melts in the sub-cratonic mantle.

Melts in equilibrium with garnet rims have been calculated for heterogeneous garnets and are summarized in Fig. 4 (Fig. 4a specifically shows the melts in equilibrium with the average rim compositions of the garnets illustrated in Fig. 3). The calculated melts show a systematic decrease in chondrite-normalized concentrations from LREE to HREE, i.e. the compositions are LREE enriched. With decreasing pressure–temperature (depth) of samples, equilibrium melt compositions show a progressive increase in LREE/HREE ratio. The deepest samples, such as JJG115 (with Type II chemical variation), show LREE <100 times chondrite and HREE at 1–10 times chondrite (Fig. 4a). Melts in equilibrium with garnets showing the major Type Ia chemical variation (J110, J107, J22 in Fig. 4a, in order of decreasing depth) show a progressive increase in LREE and decrease in HREE with depth. Thus melt in equilibrium with the J110 garnet rim has La slightly above 100 times chondrite and Lu near 0·9 times chondrite, whereas J22 has La at 300 times chondrite and Lu $<0{\cdot}5$ times chondrite. Melt in equilibrium with the rim of garnet from the coarse medium-temperature sample JJG1728 continues this trend with decreasing pressure–temperature by having La at 1000 times chondrite and Lu at *c.* 0·1 times chondrite (Fig. 4a).

Figure 4a also shows the calculated REE composition of melt in equilibrium with garnet from the Cr-poor megacryst suite. The melt in equilibrium with this megacryst has a very similar REE composition to melts in equilibrium with the deepest deformed xenolith garnets, with La slightly below 100 times chondrite and Lu just above 1 times chondrite.

In Fig. 4b we plot REE melt compositions calculated to be in equilibrium with the rim compositions of all analysed garnets that show compositional zoning, using different ornaments to distinguish data in the depth-related groups of: Type II and Ib deformed garnets (deepest); Type Ia deformed garnets (intermediate depths); Type III garnets from coarse medium-temperature xenoliths (the shallowest of the xenolith groups showing zoned garnets). Here again the calculated melt compositions show a general trend with decreasing depth, becoming more enriched (higher LREE/HREE) as one goes through Types II, Ib and Ia deformed xenolith garnets to garnets in coarse medium-temperature xenoliths, as summarized in Fig. 1. For the garnet lherzolites this trend of REE rim compositions coincides with the average rim compositions becoming richer in Ca, Cr and Ti with decreasing depth (Figs 1 and 2; and Burgess & Harte, 1999).

DISCUSSION

General evidence for percolative fractional crystallization processes in the Jagersfontein mantle section

On the basis of the major and minor element composition of the Jagersfontein peridotites, Burgess & Harte (1999) suggested that the recent evolutionary history resulted from infiltration of an ultrabasic–basic melt at the base of the deformed xenolith mantle. Crystal overgrowths and changes in the major and minor element composition with depth were used to suggest that an upwelling silicate melt evolved through the mechanism of percolative fractional crystallization (Harte *et al.*, 1993). Thus compatible elements such as Fe and Mg, for which mantle peridotite provides large reservoirs, were effectively buffered by mineral–melt exchange to near constant composition; but less compatible minor elements, such as Ti, evolved to higher concentrations through the fractional crystallization of precipitated silicate phases. The evidence from garnet overgrowths for dispersed melt infiltration and percolation in the Jagersfontein section is accompanied by a lack of megascopic evidence of concentrated flow along fissures or conduits. Thus the Jagersfontein xenoliths show a pronounced lack of dyke- and vein-like bodies (Winterburn, 1987; Hops, 1989) in contrast to localities such as Matsoku (e.g. Harte *et al.*, 1987). Likewise, the eruptive polymict peridotites of Bultfontein (Lawless *et al.*, 1979; Morfi, 2001) appear to be lacking. Thus, although possibly repetitive melt injections or eruptions to different levels may affect other mantle sections, we do not consider them for the high- and medium-temperature peridotites at Jagersfontein; the evidence is for widespread percolative flow in the manner proposed by McKenzie (1989).

The REE data presented here demonstrate the compositional variation of garnet rims, and the melts calculated to be in equilibrium with them provide clear evidence of progressive melt evolution with decreasing temperature–pressure (depth) in the Jagersfontein mantle section. With decreasing depth there is a spectrum of gradually changing melt compositions, from ones similar to those crystallizing typical megacryst garnets to ones characterized by much higher LREE and La/Lu ratios. These changes in the REE are complemented by those in Ca, Cr and Ti summarized previously. Although the overall trend with decreasing

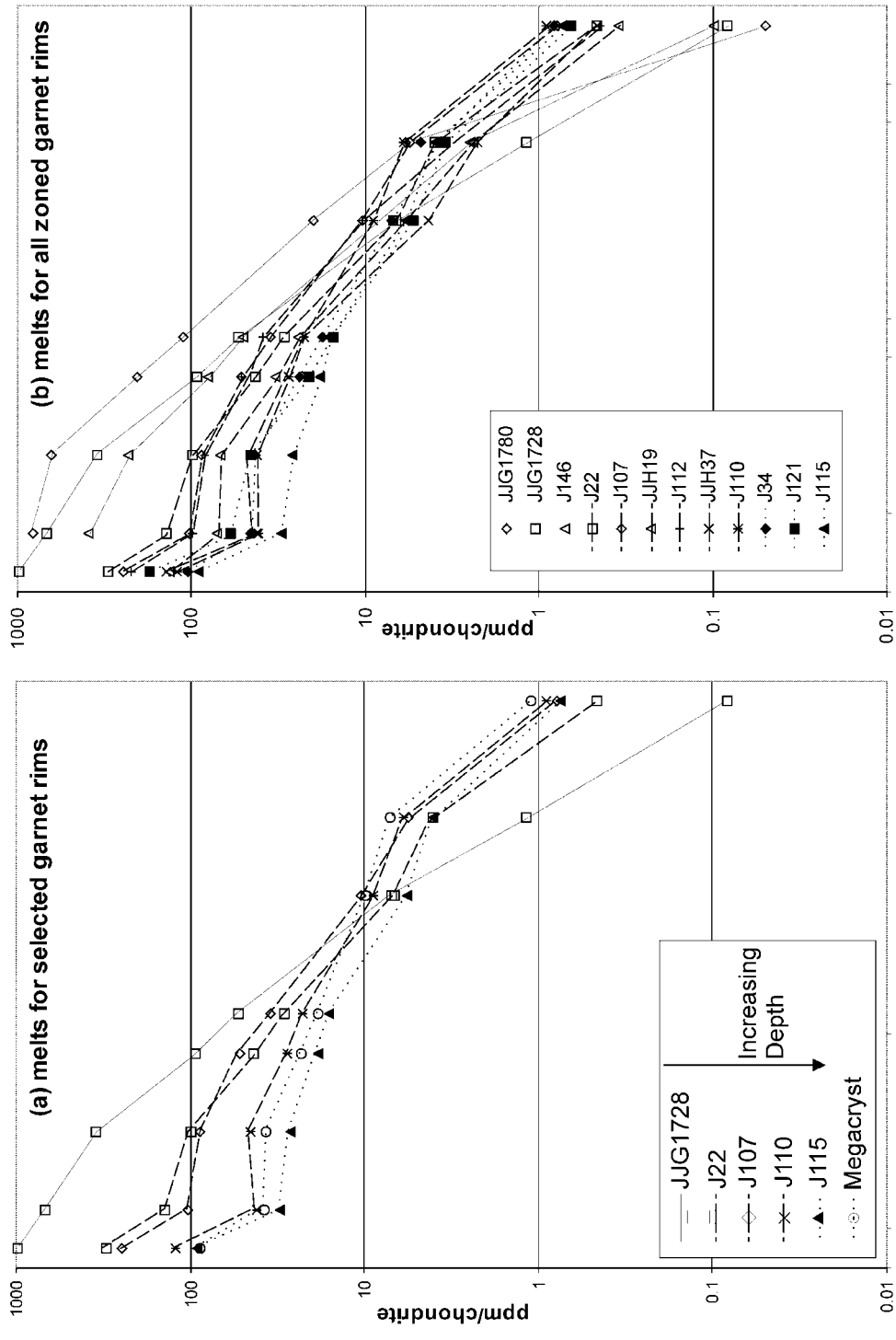

Fig. 4. Melt compositions in equilibrium with peridotitic garnet rims and garnet megacryst J75, calculated using partition coefficients of Table 3 (see text). (a) For rim compositions of garnets shown in Fig. 3; (b) for all analysed garnets showing compositional zoning. Dotted tie-lines are used for Type II and Ib garnets in deep deformed peridotites; dashed tie-lines for Type Ia garnets in shallower deformed peridotites; continuous tie-lines for Type III garnets in coarse medium-temperature peridotites. REE compositions normalized to the chondritic values of Sun & McDonough (1989).

depth is clear, at any given depth the xenoliths show evidence of a small range in melt compositions. This may be expected in a percolative fractional crystallization mechanism of melt evolution where the process is controlled by localized crystallization and chemical exchange between melt and crystals. Thus at a given depth melt compositions may vary according to variations in melt path and the extent of interaction with peridotite of individual melt batches. Evidence for such local variations is also seen in the fact that not all deformed peridotites show heterogeneous–zoned garnets and thus some appear to have escaped interaction with percolating melt. In the following sections we consider how the evolving percolative melts in the Jagersfontein peridotites relate to the melts crystallizing megacrysts and to other melts responsible for metasomatism in peridotite xenoliths from kimberlite.

The nature of melts causing metasomatism in high-temperature deformed peridotites and the melts crystallizing megacrysts

Cr-poor megacrysts from kimberlites are commonly interpreted as direct precipitates from magma bodies undergoing normal crystal fractionation in the deep lithosphere (e.g. Nixon & Boyd, 1973*a*, 1973*b*; Gurney *et al*., 1979; Harte & Gurney, 1981; Jones, 1987). It has also been advocated (Gurney & Harte, 1980; Ehrenberg, 1982; Harte, 1983; Hops *et al*., 1989, 1992; Wyllie, 1989; Harte *et al*., 1993) that melts with compositions similar to those parental to megacrysts are widely responsible for metasomatism in high-temperature deformed peridotites. This relationship is strongly supported by the detailed evidence on deformed peridotites presented here and by Burgess & Harte (1999), and in particular by the close similarity in trace elements of the calculated deepest metasomatic melt compositions and the calculated megacryst melt compositions.

Tainton & McKenzie (1994) showed a correspondence between the REE compositions of megacrysts and minerals in deformed lherzolites and those expected for minerals in equilibrium with a small fraction (0·3–0·5%) melt derived from the mid-ocean ridge basalt (MORB) source rather than an ocean island basalt (OIB) source. More consistent relationships were obtained using melt compositions calculated from clinopyroxene megacrysts than from garnet megacrysts, and Tainton & McKenzie (1994) suggested that this probably reflected some error in the garnet–melt partition coefficients used.

In Fig. 5 we plot the composition of a small fraction melt of the MORB source (McKenzie & O'Nions, 1991; Tainton & McKenzie, 1994), along with estimates of melt compositions in equilibrium with the J75 garnet megacryst from Jagersfontein. The melt compositions are calculated using: (1) the partition coefficients of McKenzie & O'Nions (1991), which are based on those of Shimizu & Kushiro (1975) and Hanson (1980); (2) the partition coefficients based on Harte *et al*. (1996) that are used generally in this paper (Table 3). It is clear that the second set of partition coefficients, despite a slightly kinked REE profile, gives a much better fit to the MORB-source melt composition. This brings the results for melts in equilibrium with megacryst garnet into correspondence with

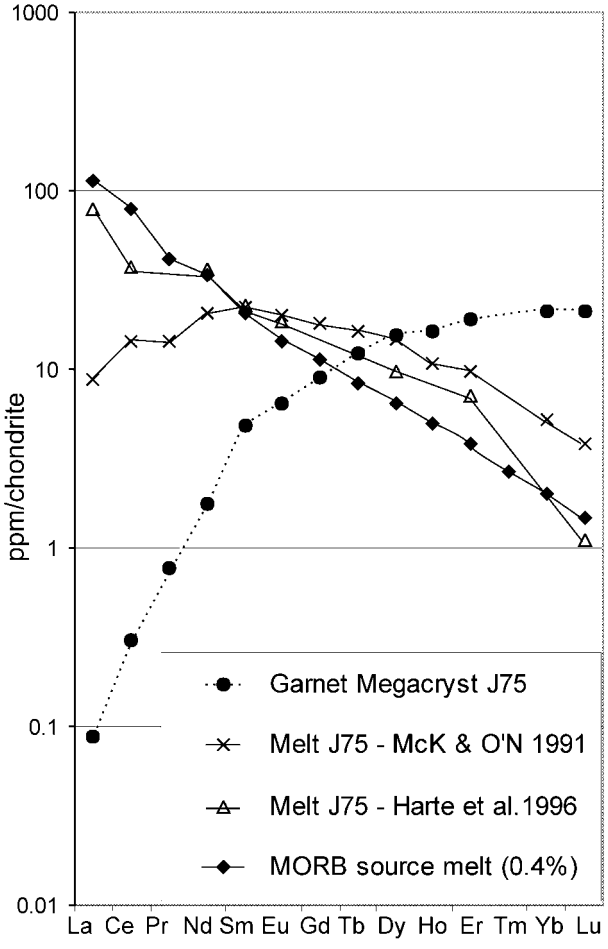

Fig. 5. Comparison of melt compositions calculated to be in equilibrium with J75 garnet megacryst. Calculations were carried out in two ways: (1) using partition coefficients from McKenzie & O'Nions (1991), following Shimizu & Kushiro (1975); (2) using partition coefficients of Table 3, based on recommendations of Harte *et al*. (1996) (see text for further details). The Harte *et al*. partition coefficients give compositions for the melt crystallizing the megacryst that are similar to those estimated for a small-volume (*c*. 0·4%) MORB-source melt (after McKenzie & O'Nions, 1991), which agrees with melt estimates based on clinopyroxene megacrysts by Tainton & McKenzie (1994).

Tainton & McKenzie's (1994) results for megacryst clinopyroxene, and agrees with the postulated linkage of megacryst magmas with asthenospheric melts and the estimated MORB-source melt compositions of McKenzie & O'Nions (1991) (see also the previous section on partition coefficients).

However, radiogenic isotope studies cast some doubt on the simplicity of this direct connection of MORB-source melts and megacryst magmas. Hops *et al.* (1992) found that $^{87}Sr/^{86}Sr$ and $^{143}Nd/^{144}Nd$ in Jagersfontein megacrysts showed more diversity than that compatible with a single MORB source, and that some source material had undergone enrichment processes that had led to higher $^{87}Sr/^{86}Sr$ and lower $^{143}Nd/^{144}Nd$ ratios. Similarly, Nowell *et al.* (1999) found that two ilmenite megacrysts from Monastery have $^{176}Hf/^{177}Hf$ signatures that require an ancient melting event in the presence of residual garnet followed by long-term isolation from the MORB source. Thus, although trace element compositions of megacrysts may be broadly compatible with a MORB-source origin for their parental melt, their isotopic compositions show evidence for a more complex history.

The manner of formation of the deformed mantle sampled by xenoliths, and whether it should be considered as part of the lithosphere or asthenosphere, has long been a matter of debate (e.g. Boyd, 1973, 1987; Nixon & Boyd, 1973*a*, 1973*b*; Green & Gueguen, 1974; Parmentier & Turcotte, 1974; Harte, 1978; Mercier, 1979; Gurney & Harte, 1980; Richardson *et al.*, 1985; Pearson *et al.*, 1995*a*). Harte (1983) and Harte & Hawkesworth (1989), in reviews of models for the deformed xenoliths, emphasized the evidence for both recystallization and metasomatism in their origin, and favoured the idea that they represented lowermost lithospheric material that had been given more fertile, asthenospheric, major and minor element characteristics by infiltration of melts from the asthenosphere (or MORB source). Further evidence for metasomatism has accumulated (e.g. Smith & Boyd, 1987; Griffin *et al.*, 1989; Hops *et al.*, 1989; Burgess & Harte, 1999), and at the same time isotopic data on the high-temperature deformed peridotites have lent further support to a mixed origin. Nd and Sr isotope characteristics (Richardson *et al.*, 1985) point to a dominantly asthenospheric source, whereas Os isotopic compositions show clear distinction from the asthenosphere and evidence of lithosphere formation in the Late Archaean or Early Proterozoic (Pearson *et al.*, 1995*a*).

Therefore, the deformed peridotite part of the mantle section may be viewed as a zone of the lowermost cratonic lithosphere, retaining some ancient distinctive isotopic features, but affected by uprising small-volume melts derived from a MORB-type source and thereby acquiring some trace element and isotopic signatures compatible with an asthenospheric origin. In conjunction with undergoing metasomatism by infiltration of uprising melt, the deformed lower-lithosphere material (with variable isotopic characteristics) probably undergoes some partial melting, as seen in the Jagersfontein xenoliths with Type II garnet zoning (Burgess & Harte, 1999), and thereby contributes to the magma that also gives rise to megacrysts. Altogether, the result of these interactions will be deformed peridotites and megacrysts that show varying extents of isotopic distinction to the MORB source, but that have a general REE signature related to that of MORB-source melt. The formation of MORB-source melt and the initiation of melting in the lowermost lithosphere are presumed to result from the development of an upward convective limb (plume in convective terms) of the asthenospheric convective circulation. This causes small-volume melt formation by giving a small rise in temperature and increase in volatile content in the uppermost asthenosphere and lowermost lithosphere (e.g. Green & Gueguen, 1974; Parmentier & Turcotte, 1974; Wyllie, 1989; Wyllie & Ryabchikov, 2000).

The role of melt–matrix exchange in the evolution of melt and mineral compositions

The importance of exchange reactions between melt and the mineral matrix or rock through which it is moving has been emphasized and modelled through consideration of chromatographic or relative incompatibility effects (e.g. McKenzie, 1984; Navon & Stolper, 1987; Bodinier *et al.*, 1990; Nielson & Wilshire, 1993; Vernières *et al.*, 1997; Ionov *et al.*, 2002*a*, 2002*b*). With respect to peridotite xenoliths from kimberlites, the importance of such exchange in the buffering of melt Mg/(Mg + Fe) ratios has been particularly emphasized (Harte, 1983; Burgess & Harte, 1999).

Exchange and reactive porous flow models have been proposed for a variety of situations and have undergone considerable development in recent years. Navon & Stolper (1987) treated the mantle as a chromatographic column with melt percolating upwards through the rock or mineral matrix and interacting with the matrix by exchange. In such a model differences in element behaviour occur because of the differing compatibilities of elements between melt and matrix; thus the solid matrix has more control over compatible than incompatible element signatures as the melt moves through it, whereas the percolating melt correspondingly controls incompatible element signatures over a greater distance than compatible ones. These effects have clear application to the Jagersfontein situation, but the Navon & Stolper model does

not consider the effects of crystal fractionation during percolation, and there is clear evidence that this has also been important in the Jagersfontein mantle section (Burgess & Harte, 1999). In the Nielson & Wilshire (1993) model the melt transfer occurs dominantly along fractures around which buffered rock zones develop. As there is a widespread lack of veins or dykes in the Jagersfontein xenoliths (Winterburn, 1987; Hops, 1989), it does not fit the geometrical relations of the Nielson & Wilshire (1993) conduit-oriented model, which seems more appropriate for situations such as that shown by Matsoku xenoliths (Harte *et al.*, 1987). More recently, Bedini *et al.* (1997), Vernières *et al.* (1997) and Ionov *et al.* (2002*a*, 2002*b*) have developed a sophisticated plate model, in which a variety of melting, compaction, crystallization and mineral–melt exchange processes are considered.

Melt–mineral exchange reactions, which are essential to the chromatographic or reactive porous flow models of Navon & Stolper (1987) and Vernières *et al.* (1997), are clearly relevant to the development of garnet rims in the Jagersfontein situation. Thus Burgess & Harte (1999) contrasted the behaviour of Mg/(Mg + Fe) ratios (extensively buffered by the complete set of mantle minerals) to the behaviour of Ti (relatively incompatible and unbuffered by peridotite) during the growth of the garnet rims. However, it is also clear from the garnet composition profiles documented by Burgess & Harte (1999) that the amount of exchange between the original garnet cores and the melt was very limited. Therefore in the following section we place emphasis on the mineral precipitation effect embodied in the growth of the garnet rims. This effect amounts to one of melt fractionation as the garnet precipitates and the melt moves upwards, and may be modelled for the REE by a Rayleigh fractional crystallization process. With this model the cumulative effect of garnet crystallization throughout the peridotite column is determined. This approach differs from the Vernières *et al.* (1997) plate model where the peridotite column is divided into a series of cells or subsystems and local equilibration takes place in each of the cells in turn. Clearly, such equilibration did not take place in the Jagersfontein case.

The role of fractionation in the evolution of metasomatic melt and mineral compositions

In the following, the effects of Rayleigh fractional crystallization on melt and mineral REE compositions are considered first for the case of garnet crystallization alone. We then proceed to consider the effects of crystallization of other minerals (olivine and pyroxenes). This is because we presume these minerals are likely to have crystallized from the melt even though widespread recrystallization of the matrix of the peridotites has removed any petrographic or compositional zoning record.

The choice of an initial melt composition for the modelling is based on the major and minor element compositions (Burgess & Harte, 1999) and the trace element data presented above. As discussed in preceding sections, these data point towards a melt composition in equilibrium with the common Cr-poor megacryst mineral compositions, and this is similar to a 0·3–0·5% fraction melt of the asthenospheric MORB source. Therefore, the melt from which garnet megacryst J75 crystallized (Figs 4 and 5) is used here as a source composition for the metasomatic melt undergoing fractionation.

Figure 6a shows the result of fractional crystallization of a megacryst melt, where the sole phase to crystallize is garnet. This plot gives the REE composition of the melt, after successive steps of 20% crystallization, from the original melt composition (labelled 1), through to the composition when 80% of the melt has crystallized garnet (labelled 0·2 for the melt fraction remaining). Figure 6b shows the composition of garnet in equilibrium with each of these calculated melt compositions. The garnet–melt partition coefficients used are those for 1300°C in Table 3. The results of this model show that fractionation of garnet from a starting megacryst melt composition causes progressive increase in LREE and decrease in HREE. Garnet–melt partition coefficients for REE from La to Eu are less than unity (Table 3), and therefore these elements are increasingly concentrated in the melt. REE from Dy to Lu, however, have garnet–melt partition coefficients greater than unity, and they are therefore concentrated in garnet and progressively depleted in melt as crystallization proceeds. Thus the effect of garnet fractionation is to greatly increase the La/Lu ratio of the melt and the slope of the REE pattern (Fig. 6a). The corresponding sequence of garnets (Fig. 6b) crystallizing from the differentiating melt show a progressive change from continuously positive curves of increasing abundance with decreasing ionic radius (or increasing atomic weight), to ones showing a maximum (or hump) of abundance within the HREE or MREE. The magnitude of the maximum increases with fractionation, and the maximum moves from the HREE towards the LREE with increasing crystallization. This humped profile in the later crystallizing garnet arises because of the strong removal of HREE from the melt by the early crystallizing garnet.

Other Rayleigh fractional crystallization models of melt compositions from the J75 initial melt composition are presented in Fig. 6c and e for clinopyroxene

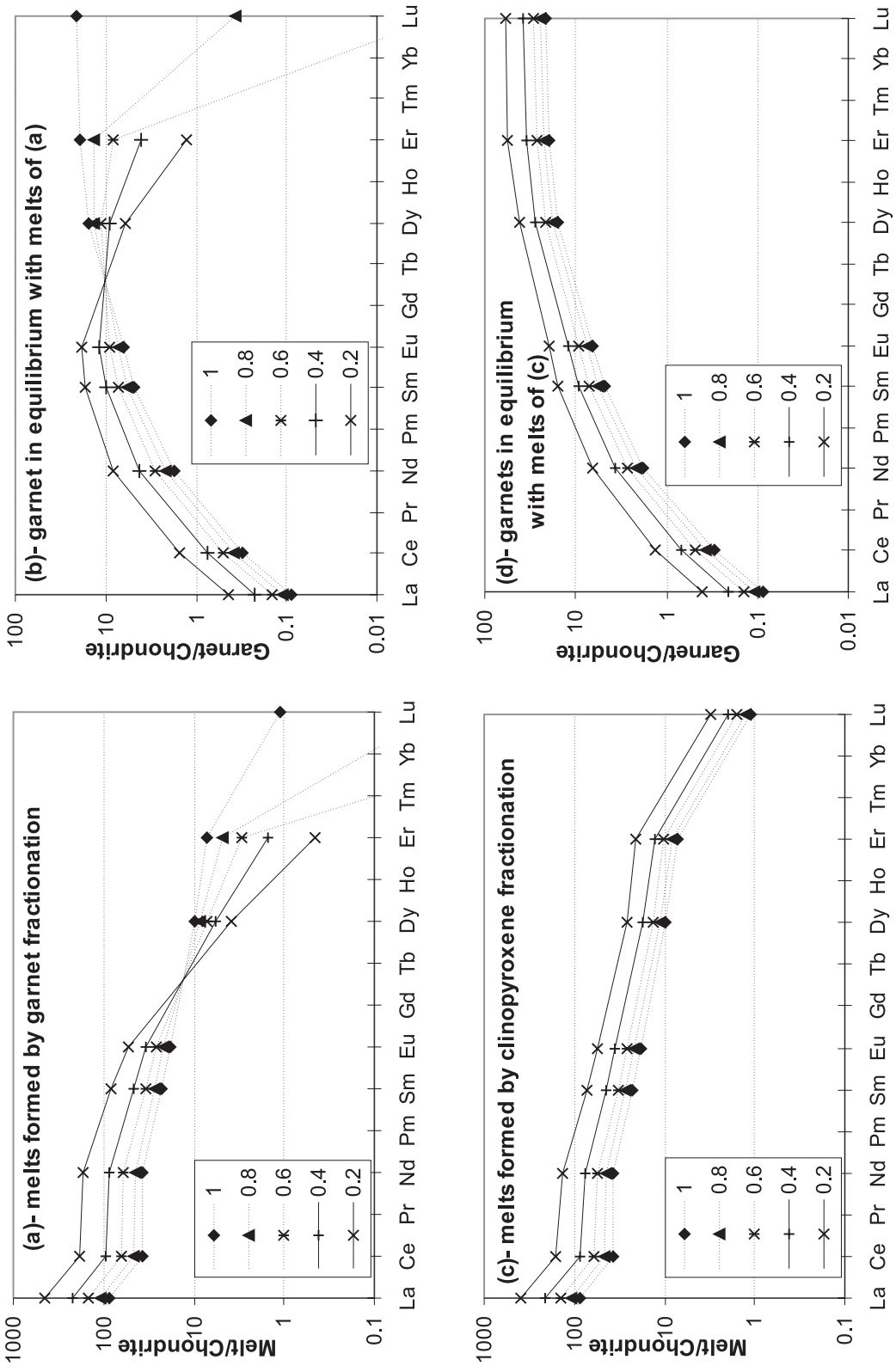

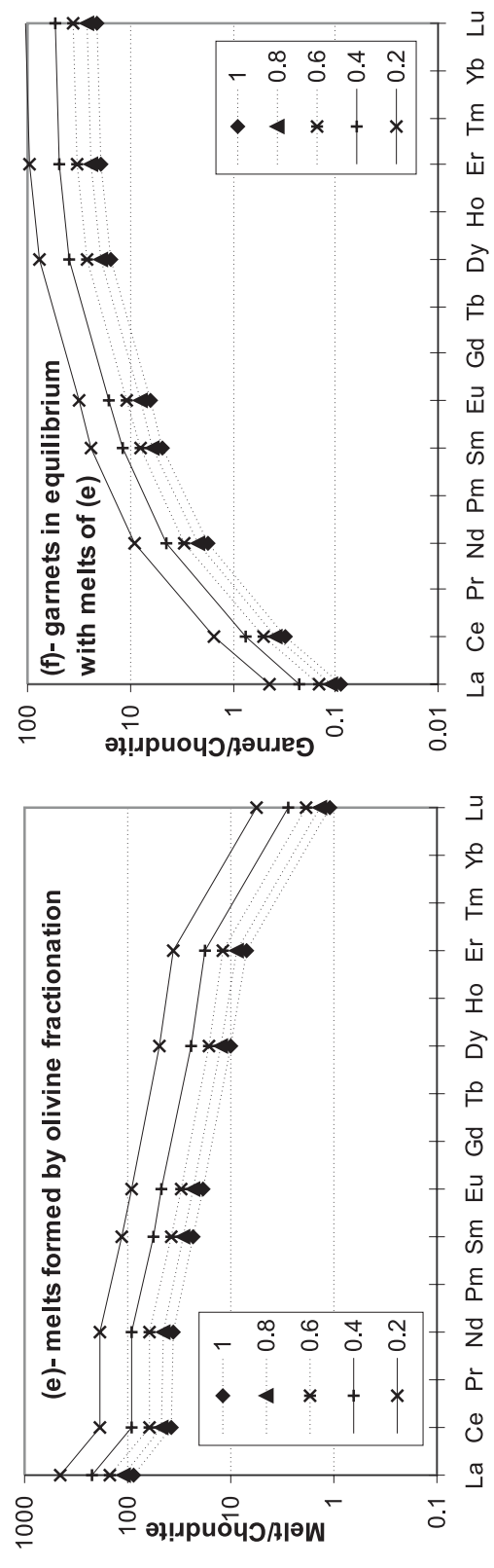

Fig. 6. (opposite) Calculated REE compositions of melts and garnets under various circumstances of fractional crystallization. There are four pairs of diagrams, with one diagram of each pair giving melt compositions and the other giving the garnet compositions corresponding to each melt. The crystals undergoing fractionation in each pair of diagrams were as follows: (a, b) garnet fractionation; (c, d) clinopyroxene fractionation; (e, f) olivine fractionation; (g, h) fractionation of a crystal mixture of 50% olivine, 25% garnet and 25% clinopyroxene. All fractionated melt compositions have been calculated using an initial melt composition (labelled 1) that would be in equilibrium with the J75 garnet megacryst (see Figs 3–5). Successive melt compositions are shown for progressive removal of crystals at 20% intervals in a Rayleigh fractionation model, and are labelled 0·8, 0·6, 0·4, 0·2. The compositions of garnets were calculated as those in equilibrium with the various fractionated melts using partition coefficients for 1300°C given in Table 3. REE compositions normalized to the chondritic values of Sun & McDonough (1989).

and olivine fractionations, respectively. The partition coefficients used for these models are again given in Table 3 (with the olivine–melt partition coefficient for La assumed to be the same as that for Ce, whereas that for Lu is assumed to be the same as that for Yb). Fractionating clinopyroxene, with cpx–melt partition coefficients <1·0 for all elements, has the effect of increasing the content of all the REE in the remaining melt. The chondrite-normalized pattern is little altered in shape (the La/Lu ratio remains little changed), but it moves to higher relative concentrations with progressive fractionation (Fig. 6c). As a consequence, clinopyroxene fractionation has little effect on the shape of the REE pattern (Fig. 6d) of garnets in equilibrium with the resultant melts. The REE composition of garnet simply increases with progressive fractionation for all elements.

The results for olivine fractionation (Fig. 6e and f) are similar to those of clinopyroxene, but are more extreme as the olivine–melt partition coefficients are lower than those of clinopyroxene. Thus the REE are concentrated more effectively into the evolving melt. Again, the shape of the REE pattern of the melts (Fig. 6e) and the garnets (Fig. 6g) in equilibrium with the melts does not change significantly. The effects of orthopyroxene fractionation alone are not illustrated in Fig. 6. This is because the orthopyroxene–melt partition coefficients (given in Table 3) have values between those of olivine–melt and clinopyroxene–melt. Therefore, REE changes during fractionation of orthopyroxene are intermediate between those shown in Fig. 6c and Fig. 6e.

The above modelling shows the unique importance of garnet fractionation in changing the relative pattern of abundance of the REE in the evolving melts. However, the process of garnet fractionation is likely to have been accompanied by that of olivine and pyroxenes, although it cannot be documented by zoning relationships in the deformed peridotites because of the extensive recrystallization of these phases during deformation.

Figure 6g represents a fractional crystallization model involving the crystallization of olivine:clinopyroxene:garnet in the ratio 2:1:1 over the entire fractionation sequence (orthopyroxene is not treated separately, as we have seen that its effects are similar to a combination of clinopyroxene and olivine). The melts in Fig. 6g show the pattern of LREE enrichment seen in Fig. 6a and the melts calculated from the actual garnet rims (Fig. 4). However, the quantitative fit for the HREE in particular has two weaknesses. First, unlike the garnet-only fractionation model, only the heaviest REE become depleted in the melt where other phases are crystallizing. Second, the modelled depletion of Lu is more extreme than that indicated from the melts in equilibrium with the Jagersfontein samples. The effect in terms of the modelled garnet compositions (Fig. 6h) is that the peak or hump in the REE pattern for more fractionated compositions is in the HREE and not in the MREE.

These weaknesses in the modelling may be partly connected with the partition coefficients adopted. Although the garnet–melt partition coefficients based on Harte *et al.* (1996) are more compatible with other data (see previous discussion), the garnet–melt D for Lu still appears to be too high and those of Er and Dy perhaps too low. Support for these inferences is given by the occurrence of similar irregularities in comparing calculated megacryst melts with those from the MORB source (Fig. 5). Other factors that may affect the partition coefficients are the effects of falling temperature and changing major–minor element compositions as the percolating and fractionating melt moves upward. Temperature dependence is hard to evaluate given the lack of data on mineral–melt partition coefficients as a function of temperature alone. With respect to composition, Harte & Kirkley (1997) have shown that major element chemistry, and in particular increasing Ca, may have a dramatic effect on increasing the relative compatibility of lighter REE to heavier REE in the garnet crystal structure. Thus it is possible that as Ca increases in the peridotite garnets along the lherzolite line (Fig. 2), the division between compatible and incompatible behaviour for garnets moves to lighter REE and the contrast in partition coefficients between Lu and other REE decreases. This will then affect the position and magnitude of the maximum in the humped REE patterns (Figs 3 and 6).

None the less, the modelled compositions shown in Fig. 6 exhibit important features in common with the observed compositions seen in the Jagersfontein samples (Figs 3 and 4). Thus garnet crystallization or fractionation in the model has the important effect of greatly changing LREE/HREE ratios in the evolving melts and gives rise to melts that crystallize garnets with humped REE patterns, as seen in the natural samples. Crystallization or fractionation of olivine and pyroxenes causes little relative change in LREE/HREE and therefore subdues the effect of garnet on the melt REE profile, but they do have the important effect of increasing the total REE content of the melt. Fractionation of olivine and orthopyroxene, because of their low REE contents, will be particularly important in explaining REE increases in derived melts. It may be noted that the presence of additional phases, such as amphibole and phlogopite, would not strongly modify these results for the REE, as their relative REE abundances are largely similar to combinations of olivine and pyroxenes (Kramers *et al.*, 1983; Witt-Eickschen & Harte, 1994).

Melt differentiation and the formation of humped REE profiles in garnet

Shimizu & Richardson (1987) and Hoal *et al*. (1994) have drawn attention to the extreme trace element enrichment (as defined by high concentrations of LREE and high LREE/HREE ratios) implied by humped or sinusoidal garnet patterns, which are common in some modally metasomatized peridotites and in peridotitic-suite garnet inclusions in diamonds. They have pointed out that calculated melt compositions in equilibrium with coarse garnet showing humped REE patterns are unlike those of any known type of melt erupted at the Earth's surface, including kimberlites and carbonatites. This lack of correspondence in trace element characteristics between calculated melt compositions and actual melts erupted at the surface has led to hypotheses that the extremely evolved humped REE patterns cannot be the result of garnet–melt equilibria. Thus it has been suggested that they imply a disequilibrium process, which may also give rise to unusual and variable Cr and Ti distributions (e.g. Shimizu & Richardson, 1987; Hoal *et al*. 1994).

More recently, the occurrence of small-scale spatial variations in trace element distribution in garnets showing humped REE patterns has provided other evidence of disequilibrium, and decreasing rates of diffusion in the REE with decreasing ionic radius have been particularly suggested as the main cause of this disequilibrium within the REE (e.g. Shimizu & Sobolev, 1995; Shimizu *et al*., 1997, 1999; Shimizu, 1999). However, Griffin *et al*. (1999*b*) have commented that the present data on REE diffusion coefficients do not support this hypothesis, and they have put forward the alternative suggestion that the humped patterns reflect changes in partition coefficients in garnets with low Ca content. Harte & Kirkley (1997) provided evidence of changing partition coefficients with garnet Ca content, but the changes occurring from LREE to HREE appear gradual and not of the correct magnitude to generate the humped profiles. Also in the case of JJG1728, documented in this paper (Fig. 3f), strongly humped profiles occur in garnet cores and rims that have widely different Ca contents (Fig. 2).

As an alternative to the above suggestions, we have shown (see particularly Figs 3, 4 and 6) that humped (or sinusoidal) garnet patterns may result by crystallization from melts that have undergone garnet fractionation. In the process of percolative fractional crystallization envisaged, local crystal–melt equilibrium is maintained in discrete small parts of the rock–melt column (as in a chromatographic column), with the general geochemical direction of melt evolution controlled by its progressive upward movement. The lack of overall equilibrium will allow localized variations in features such as the REE, Cr and Ti contents. With respect to the argument of Shimizu & Richardson (1987) that the extremely enriched calculated melt compositions are unreasonable because they do not match those of melts erupted at the Earth's surface, we suggest that it is not necessary for such melt compositions ever to reach the Earth's surface in discrete melt bodies. McKenzie (1989) has shown from thermal considerations that entire bodies of percolating small fraction metasomatic melts are unlikely to escape from the mantle.

Thus we emphasize the results of the earlier sections that enriched melts in equilibrium with garnets with humped REE patterns can be produced by fractionation of garnet and other normal peridotite minerals from a common megacryst melt. We believe the 'humped' REE garnet pattern can be in equilibrium with the fractionated melt, and note that a 'humped' garnet profile does not necessitate humped profiles in melt or phases such as clinopyroxene in equilibrium with it. The humped profile is a product of the unusual situation that a change from incompatible to compatible behaviour for garnets lies within the REE spectrum.

Melt–fluid compositions responsible for modal metasomatism and isolated trace element enrichment

Many studies have been concerned with the compositions of fluids responsible for both modal mantle metasomatism (typically where new mineral phases, such as amphibole or phlogopite, are formed in the rocks) and isolated trace element enrichment (unaccompanied by modal or major–minor element changes) [see, for example, the collection of papers in the book by Menzies & Hawkesworth (1987) and the review by Harte & Hawkesworth (1989)]. The view has widely developed, particularly from trace element and isotope considerations, that the melts or fluids responsible for modal metasomatism may evolve by interaction with peridotite to cause isolated trace element enrichment in other peridotites (e.g. Harte, 1983; Menzies *et al*., 1985; Wilshire, 1987; Bodinier *et al*., 1990; Harte *et al*., 1993).

The detailed sequence of melt REE compositions (Fig. 4) obtained from the Jagersfontein mantle section has a range that covers a variety of metasomatic melt compositions documented for other localities. The calculated melt compositions in Fig. 4 overlap with those appropriate for isolated trace element enrichment in many coarse xenoliths. The more evolved calculated REE compositions are similar to those associated with modal metasomatism involving amphibole (with or

without phogopite), which is found in low-temperature coarse peridotite xenoliths—examples include the metasomatism related to the MARID suite described by Dawson (1987), Erlank *et al.* (1987) and Hoal *et al.* (1994); and the edenitic amphibole metasomatism of Field *et al.* (1989) and Winterburn *et al.* (1990). Thus the present data support the view that a variety of metasomatic melts may have a similar source and that their varied nature is the result of varying degrees of differentiation during percolative fractional crystallization or porous reactive flow. In effect, this means that many of the melts interacting with lower cratonic lithosphere peridotites have a similar source to the melts crystallizing common Cr-poor megacrysts.

Evidence for earlier and multiple episodes of melt migration and metasomatism

The emphasis of this paper has been upon the rim compositions of garnets from Jagersfontein and how they change in relation to the pressure–temperature (depth) relationships of the peridotites. However, Fig. 3 shows that the core compositions are not constant. Instead, they show a sequence of depth-related changes, which mirror many of the changes in rim compositions. Indeed, at any given depth, the cores tend to be more enriched (with higher La/Lu) than the rims. In Fig. 7 melt compositions, calculated to be in equilibrium with the garnet core compositions, show a sequence of increasing LREE concentrations and LREE/HREE ratios with decreasing depth, similar to that of the melts calculated to be in equilibrium with the garnet rims (Fig. 4). The only difference is that the melts in equilibrium with the garnet cores extend to more enriched compositions. It should be noted that this sequence of core compositions is considered to belong to a distinct event from that responsible for rim compositions, because cores and rims often show relatively abrupt interfaces with limited diffusional transfer (Burgess & Harte, 1999).

Thus, there is clear evidence from garnet core compositions that prior to the infiltration event that formed the garnet rims peridotite garnets already showed a progression to more enriched compositions with decreasing depth. This implies the probability of more than one metasomatic infiltration event in the Jagersfontein mantle section. At any given depth these earlier melts must have had a more evolved REE signature than the more recent melts, and the earlier melts therefore generated the extremely evolved humped garnet compositions of the medium-temperature coarse G10 garnet harzburgites (e.g. JJG1728; see Figs 2, 3 and 7).

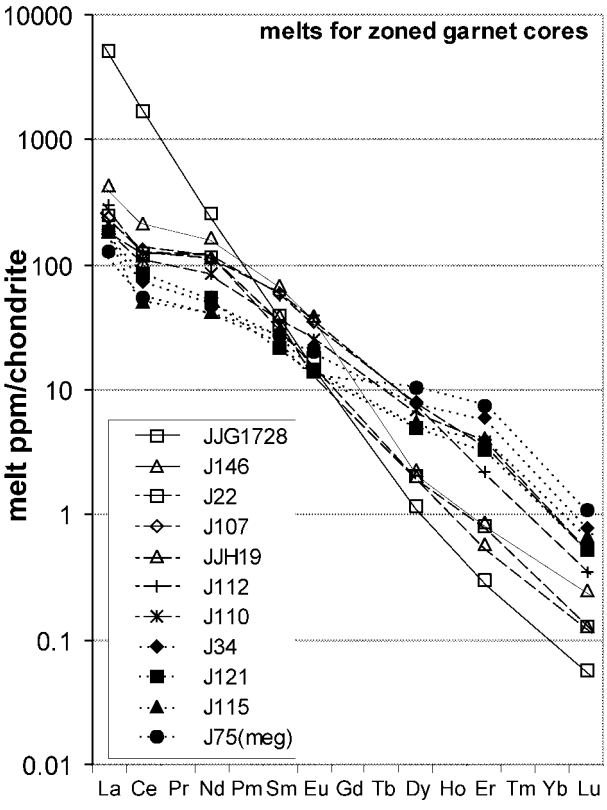

Fig. 7. Melt compositions in equilibrium with peridotitic garnet cores, calculated using partition coefficients of Table 3, and normalized to the chondritic values of Sun & McDonough (1989). Compositions are for equilibrium with average garnet cores of the same specimens given in Fig. 4. Dotted tie-lines are used for Type II and Ib zoned garnets in deep deformed peridotites; dashed tie-lines for Type Ia zoned garnets in shallower deformed peridotites; continuous tie-lines for Type III garnets in coarse medium-temperature peridotites. The melt composition in equilibrium with garnet megacryst J75 is given for comparison.

The occurrence of the diamond–garnet harzburgite paragenesis

Burgess & Harte (1999) provided clear evidence from major and minor element compositions for the modification of deformed and coarse garnet harzburgites (with G10 garnet compositions) towards the lherzolite compositional trend (with G9 garnets). A particularly large change in garnet CaO composition, from well inside the G10 field, is illustrated by coarse harzburgite JJG1728 in Fig. 2. In other cases (e.g. deformed harzburgite J22), a small change in garnet CaO brings the garnet to the lherzolite trend, and then zoning becomes Type Ia along the lherzolite trend. In terms of REE, the major and minor element zoning is accompanied by a shift of the hump in the REE pattern towards the HREE (as a result of LREE subtraction and HREE addition), and may lead to the HREE-enriched

plateau pattern typical of many deformed G9 garnets on the lherzolite trend (Fig. 3). This chemical change appears to be driven by the growth of garnet from a melt that has been buffered to a lherzolite composition by extensive percolation through lherzolites at lower levels. In JJG1728 it is estimated that as much as 70% of the volume of the garnet represents rim overgrowth on G10 cores (Burgess, 1997). It is possible that some of the Jagersfontein lherzolites, marked by a combination of very small amounts of clinopyroxene and relatively high-Cr garnets, could formerly have been G10 harzburgites.

In parallel with these observations, Griffin *et al.* (1999*b*) described zoned garnets in which the major variation is from Ca poor (harzburgitic) to Ca rich (lherzolitic). Schulze (1995) and Boyd *et al.* (1997) also drew attention to cases in which clinopyroxene is precipitated in garnet harzburgites and effects a conversion to lherzolites. In these cases, those researchers attributed the metasomatic conversions to local effects, but this does not exclude the possibility that they formed part of wider-scale metasomatic melt percolation processes similar to those documented for the Jagersfontein xenoliths.

The question clearly arises of the relevance of the above metasomatic changes to the long-term preservation of G10 garnets and, in particular, the garnet harzburgite parageneses that are indicated frequently in peridotitic diamond inclusions (Sobolev, 1977; Gurney, 1984) and appear to come from the cratonic root zone (Boyd & Gurney, 1986; Boyd *et al.*, 1993). The paragenesis commonly shown by peridotite suite inclusions in diamonds is in fact a very distinctive one, with high Mg/(Mg + Fe) in olivine, orthopyroxene and garnet, coupled with typical garnet Cr_2O_3 and CaO of 8·0–13·0 and $<2{\cdot}5$ wt %, respectively. The G10 garnet compositions are therefore extreme in themselves, having the highest Cr_2O_3 and lowest CaO known (Gurney & Switzer, 1973; Sobolev, 1977; Gurney, 1984), and we use the term 'diamond–garnet harzburgite paragenesis' to refer specifically to the suite of very depleted inclusion compositions associated with such garnets. Peridotite xenoliths generally do not show this specific diamond–garnet harzburgite paragenesis. In South Africa, the closest approach to xenoliths showing this paragenesis is provided by a suite of diamondiferous garnet-rich xenoliths and garnet macrocrysts from the Newlands kimberlite pipes (Menzies *et al.*, 1999).

Nd model ages of composites of garnet inclusions from diamonds from the Finsch and Kimberley pipes range from 3·2 to 3·5 Ga, depending upon whether they are referred to Bulk Earth or depleted mantle reservoirs (Richardson *et al.*, 1984; Pearson & Shirey, 1999). For the South African Newlands assemblages, bulk Re–Os data give ages in excess of 2·5 Ga (Menzies *et al.*, 1999). A suite of diamondiferous garnet harzburgites and dunites from Siberia also give ancient Re–Os model ages of 3·1 Ga (Pearson *et al.*, 1995*b*). These Archaean ages specifically embrace the diamond–garnet harzburgite inclusion paragenesis with highly depleted G10 garnets rather than a spread of G10 compositions (e.g. Richardson & Harris, 1997). There are also distinct differences in Nd and Sr isotope ratios between the diamond–garnet harzburgite inclusion garnets and the G10 garnets found widely in concentrate or xenoliths. Thus, although model ages are subject to uncertainties [see review by Pearson & Shirey (1999)], there is definite evidence that the specific diamond–garnet harzburgite paragenesis is distinct and of Archaean age.

Despite the depleted major and minor element compositions of the diamond–garnet harzburgite paragenesis, the garnet REE show extremely enriched compositions in terms of both Nd isotopes and LREE/HREE ratios (Richardson *et al.*, 1984; Shimizu & Richardson, 1987). This suggests a two-stage evolution for the diamond–garnet harzburgite paragenesis in which a metasomatic trace element enrichment was imposed on a previously highly depleted composition (Richardson *et al.*, 1984). In comparing garnets included in diamonds and those in harzburgite xenoliths, Gurney (1984), Nixon *et al.* (1987) and Boyd *et al.* (1993) suggested that metasomatic processes may explain the higher CaO and lower Cr_2O_3 content of G10 garnets in harzburgite xenoliths. They suggested that xenolith-hosted G10 garnets have been affected by metasomatism, from which the garnet inclusions were protected by their armour of diamond. The idea of the occurrence of metasomatism is consistent with the chemical changes identified at Jagersfontein by Boyd *et al.* (1993), and the harzburgite-to-lherzolite conversion documented in this study. However, Boyd *et al.* (1993) suggested that a problem exists in using this process to explain the restricted occurrence of the diamond–garnet harzburgite paragenesis, in that the original compositions of the xenolith-hosted G10 garnets prior to metasomatism appear to be richer in Ca than those typical of diamond-inclusion garnet chemistry.

We believe that the Jagersfontein evidence strongly supports the idea that since formation of the diamond–garnet harzburgite paragenesis under special circumstances in the Archaean, it has been progressively removed in peridotitic rocks by repeated episodes of metasomatism caused by infiltrating low-volume lherzolitic melts. At Jagersfontein there is not only evidence of the harzburgite to lherzolite conversion by metasomatism, but that more than one period of melt infiltration may have moved the composition of G10 garnets towards the G9 trend. Such multiple events of meta-

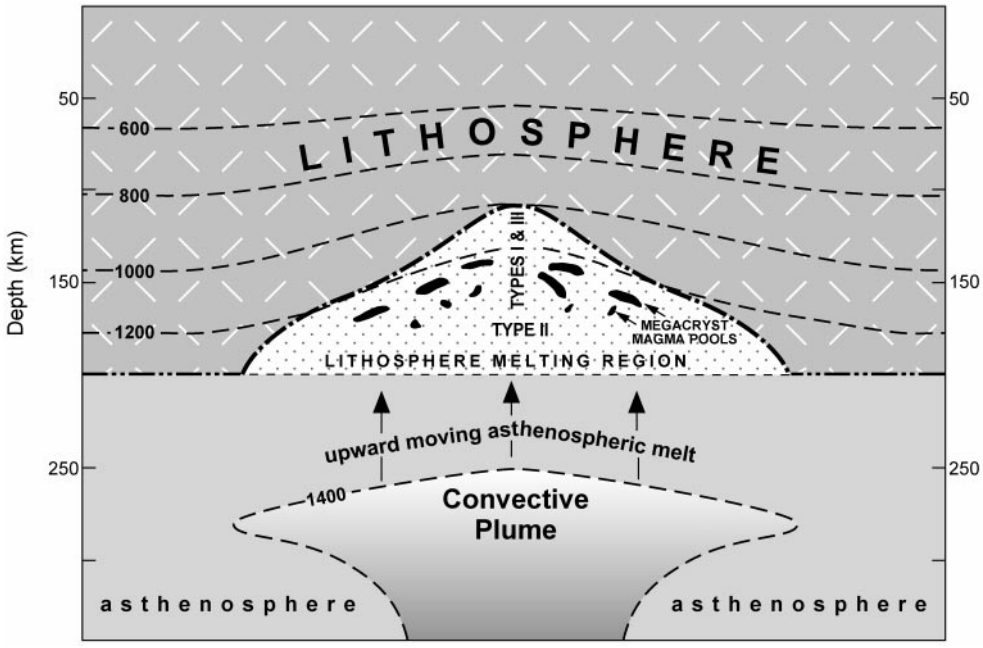

Fig. 8. Schematic portrayal of the interpretation of the Jagersfontein peridotite xenolith and megacryst section at the time of sampling by kimberlite; based upon the features described herein (see also Hops *et al.*, 1992; Burgess & Harte, 1999) and upon melting relationships summarized by Wyllie (1989) and Wyllie & Ryabchikov (2000). The central axis of the diagram summarizes the features indicated by the Jagersfontein peridotites with a zone of dispersed melt (dotted region) up to *c.* 110 km. The temperature–pressure gradient along this line is based upon the conductive–convective geotherm model of McKenzie (1989). The temperature–depth gradients at the sides of the diagram approximate those of normal cratonic lithosphere and are perturbed in the central region as a consequence of a convective plume (Green & Gueguen, 1974; Parmentier & Turcotte, 1974). Above the plume a small rise in temperature accompanied by an increase in volatile content (Wyllie, 1989; Wyllie & Ryabchikov, 2000) leads to partial melting in the uppermost asthenosphere and lowermost lithosphere. Garnet types are defined by Burgess & Harte (1999) and are summarized in the text. Type II zoned garnets are associated with melting at the greatest lithosphere depths; Types I and III garnet rims crystallize in the region of megacryst magma pools and up to the highest levels of melt percolation.

somatism counter the concerns of Boyd *et al.* (1993) that there is insufficient evidence for a large change in garnet Ca contents with metasomatism. Thus the reason for the extensive restriction of the Cr-rich diamond–garnet harzburgite paragenesis to diamonds is that it has been widely modified where not protected by encapsulation in diamonds. It may be noted that these ideas are in harmony with the broad suggestions of Griffin *et al.* (1999*a*) that the sub-continental lithosphere mantle has undergone a progression from more depleted to more fertile compositions with time.

CONCLUSIONS

The REE compositions of garnets in mantle peridotite xenoliths from the Jagersfontein kimberlite pipe vary both within individual grains in one xenolith and between garnets from different xenoliths. These variations are spatially related to major and minor element zonation patterns in individual garnets and show systematic changes with depth of origin of the peridotite xenoliths as determined by thermobarometry (Burgess, 1997; Burgess & Harte, 1999).

The garnet rims provide evidence of a widespread event of garnet growth on pre-existing garnet cores in deformed peridotites and the deeper-level coarse peridotites over a depth interval from *c.* 190 to 110 km (Fig. 1). The REE compositions demonstrate that these rims have grown from melts and it appears that upward melt transport at Jagersfontein was by grain-scale percolation through the peridotite host rocks rather than by concentrated flow along cracks and fissures. An extensive region of dispersed melts is postulated as summarized in Fig. 8. At the deepest levels sampled represented by peridotite xenoliths (with Type II and deep-level Type I garnet rims in Fig. 8) REE data show the melt compositions to have been closely similar to those of magmas that precipitated the common minerals (olivine, orthopyroxene, garnet and clinopyroxene) of the Cr-poor megacryst suite. These REE compositions also match those expected for small-volume (0·3–0·5%) partial melts (Tainton & McKenzie, 1994) of the asthenospheric MORB source. However, radiogenic isotope compositions (e.g. Hops *et al.*, 1992; Nowell *et al.*, 1999) show variations from MORB-source compositions to more

enriched compositions, which may be explained by melting and assimilation of deep lithospheric material as indicated in Fig. 8. This is supported by evidence of garnet resorption in the deep Type II zoned garnet profiles (Burgess & Harte, 1999).

With increasing height in the mantle, across the depth zone showing Type I and III garnet rims in Fig. 8, the melts giving rise to the garnet rims showed increasing LREE/HREE and at the highest levels were in equilibrium with garnets showing humped REE patterns (with a maximum relative to chondrite in the MREE). Modelling of the whole range of metasomatic melt compositions suggests that they evolved by a process of percolative fractional crystallization (Harte *et al*., 1993) or reactive porous flow (Bedini *et al*., 1997). As the melt percolated upwards through the peridotites it underwent fractionation by precipitating the garnet rims, probably together with olivine and pyroxenes, but was simultaneously buffered in terms of compatible major elements by the minerals in the pre-existing peridotites. Thus incompatible elements such as Ti and the REE became progressively more enriched in the melts but the melts remain in equilibrium with relatively Mg-rich major element compositions. The buffering of percolating melts with extensive garnet lherzolite in the Jagersfontein peridotite column has also caused original harzburgites (with G10 garnet compositions) to be modified toward lherzolite compositions by increases in harzburgite CaO contents.

The progressive increase of LREE/HREE in the upwardly percolating melts is largely a product of the fractionation of garnet. The crystallization of garnet rims at lower levels drives the melts towards extremely LREE-enriched and HREE-depleted compositions that then precipitate garnet rims with humped REE profiles at high levels. In this process the new garnet may grow in equilibrium with the adjacent melt, and the formation of a humped pattern does not depend on local disequilibrium.

The more evolved percolating melts documented for Jagersfontein have REE compositions similar to those documented for metasomatic fluids causing modal metasomatism (with formation of amphiboles and phlogopite) and trace element enrichment in low-temperature coarse peridotite xenoliths. Thus the melts responsible for these types of metasomatism may also be derived by differentiation from the parental melts of the Cr-poor megacryst suite. Therefore, the wide compositional range of the melts formed by percolative fractional crystallization allows links to be drawn between the crystallization of megacrysts, the compositions of minerals in high-temperature deformed peridotites, and the metasomatic and enrichment phenomena seen in low-temperature coarse peridotites.

The cores of garnets in the medium- to high-temperature Jagersfontein peridotites show that the original garnets of the peridotites also had increasing LREE/HREE with depth and may have been previously crystallized by similar differentiation processes from those documented for their rims. This suggests that the lower part of the mantle lithosphere is subjected to repeated episodes of: (1) injection or intrusion by asthenospheric (MORB-source) melts that induce melting in the basal cratonic lithosphere and form megacryst magma bodies; (2) metasomatism by upwardly percolating melts whose initial compositions are closely similar to those of the parental megacryst magmas. At Jagersfontein these processes are also seen to convert garnets from harzburgitic to lherzolitic compositions, and may therefore be responsible for the modification of Cr-rich Archaean diamond–garnet harzburgite parageneses with time.

ACKNOWLEDGEMENTS

We wish to thank John Craven, Richard Hinton, Peter Hill and Stuart Kearns for much help with ion and electron microprobe analyses. Discussions with Barry Dawson, John Gurney, Andrew Menzies and Steve Richardson have been much appreciated. Helpful reviews were provided by Jean-Louis Bodinier, William Griffin, Dmitri Ionov, Martin Menzies, Graham Pearson and Steve Richardson. Pamela Kempton is particularly thanked for her detailed and thoughtful editing. The University of Cape Town (and in particular John Gurney) is thanked for considerable help in locating and providing specimens. The work was carried out under NERC grant GR3 8562, and S.R.B. is grateful for an NERC research studentship. We are also grateful to De Beers Consolidated Mines Ltd and the 7th Kimberlite Conference Organising Committee (Cape Town) for help with field work and travelling expenses.

SUPPLEMENTARY DATA

Supplementary data for this paper are available on *Journal of Petrology* online.

REFERENCES

Bedini, R. M., Bodinier, J.-L., Dautria, J.-M. & Morten, L. (1997). Evolution of LILE-enriched small melt fractions in the lithospheric mantle: a case study from the East African Rift. *Earth and Planetary Science Letters* **153**, 67–83.

Blundy, J. D. & Wood, B. J. (1991). Crystal-chemical controls on the partitioning of Sr and Ba between plagioclase feldspar, silicate melts, and hydrothermal solutions. *Geochimica et Cosmochimica Acta* **55**, 193–209.

Blundy, J. D., Robinson, J. A. C. & Wood, B. J. (1998). Heavy REE are compatible in clinopyroxene on the spinel lherzolite solidus. *Earth and Planetary Science Letters* **160**, 493–504.

Bodinier, J. L., Vasseur, G., Vernières, J., Dupuy, C. & Fabriès, J. (1990). Mechanisms of mantle metasomatism: geochemical evidence from the Lherz orogenic peridotite. *Journal of Petrology* **31**, 597–628.

Boyd, F. R. (1973). A pyroxene geotherm. *Geochimica et Cosmochimica Acta* **37**, 2533–2546.

Boyd, F. R. (1987). High- and low-temperature garnet peridotite xenoliths and their possible relation to the lithosphere–asthenosphere boundary beneath southern Africa. In: Nixon, P. H. (ed.) *Mantle Xenoliths*. Chichester: John Wiley, pp. 403–412.

Boyd, F. R. & Gurney, J. J. (1986). Diamonds and the African lithosphere. *Science* **232**, 472–477.

Boyd, F. R., Pearson, D. G., Nixon, P. H. & Mertzman, S. (1993). Low Ca garnet harzburgites from southern Africa: their relations to craton structure and diamond crystallization. *Contributions to Mineralogy and Petrology* **113**, 352–366.

Boyd, F. R., Pokhilenko, N. P., Pearson, D. G., Mertzman, S., Sobolev, N. V. & Finger, L. W. (1997). Composition of the Siberian cratonic mantle: evidence from Udachnaya peridotite xenoliths. *Contributions to Mineralogy and Petrology* **128**, 228–246.

Brey, G. P. & Kohler, T. J. (1990). Geothermometry in four-phase lherzolites II: new thermometers and a practical assessment of existing thermobarometers. *Journal of Petrology* **31**, 1353–1378.

Burgess, S. R. (1997). The evolution of the sub-cratonic mantle seen in mantle xenoliths. Ph.D. thesis, University of Edinburgh.

Burgess, S. R. & Harte, B. (1999). Tracing lithosphere evolution through the analysis of heterogeneous G9/G10 garnet in peridotite xenoliths, I: Major element chemistry. In: Gurney, J. J., Gurney, J. L., Pascoe, M. D. & Richardson, S. H. (eds) *Proceedings of the 7th Kimberlite Conference (Dawson volume)*. Cape Town: Red Roof Design, pp. 66–80.

Dawson, J. B. (1984). Contrasting types of upper mantle metasomatism. In: Kornprobst, J. (ed.) *Kimberlites II. The Mantle and Crust–Mantle Relationships*. Amsterdam: Elsevier, pp. 289–294.

Dawson, J. B. (1987). The MARID suite of xenoliths in kimberlite: relationship to veined and metasomatised peridotite xenoliths. In: Nixon, P. H. (ed.) *Mantle Xenoliths*. Chichester: John Wiley, pp. 465–473.

Dawson, J. B. & Stephens, W. E. (1976). Statistical classification of garnets from kimberlite and associated xenoliths. *Journal of Geology* **53**, 589–607.

Dick, H. J. B. & Natland, J. H. (1996). Late-stage melt evolution and transport in the shallow mantle beneath the East Pacific Rise. In: Mevel, C., Gillis, K. M., Allan, J. F. & Meyer, P. S. (eds) *Proceedings of the Ocean Drilling Program, Scientific Results, 147*. College Station, TX: Ocean Drilling Program, pp. 103–134.

Eggler, D. H. (1987). Solubility of major and trace elements in mantle metasomatic fluids: experimental constraints. In: Menzies, M. A. & Hawkesworth, C. J. (eds) *Mantle Metasomatism*. London: Academic Press, pp. 21–41.

Ehrenberg, S. N. (1979). Garnetiferous ultramafic inclusions in minette from the Navajo Volcanic Field. In: Boyd, F. R. & Meyer, H. O. A. (eds) *Proceedings, 2nd International Kimberlite Conference, 2*. Washington, DC: American Geophysical Union, pp. 330–344.

Ehrenberg, S. N. (1982). Petrogenesis of garnet lherzolite and megacrystalline nodules from the Thumb, Navajo Volcanic Field. *Journal of Petrology* **23**, 507–547.

Erlank, A. J., Waters, F. G., Hawkesworth, C. J., Haggerty, S. E., Allsopp, H. L., Rickard, R. S. & Menzies, M. A. (1987). Evidence for mantle metasomatism in peridotite nodules from the Kimberley Pipes, South Africa. In: Menzies, M. A. & Hawkesworth, C. J. (eds) *Mantle Metasomatism*. London: Academic Press, pp. 221–311.

Field, S. W., Haggerty, S. E. & Erlank, A. J. (1989). Subcontinental metasomatism in the region of Jagersfontein, South Africa. In: Ross, J., Jaques, A. L., Ferguson, J., Green, D. H., O'Reilly, S. Y., Danchin, R. V. & Janse, A. J. A. *Kimberlites and Related Rocks, Volume 2. Australian Geological Society, Special Publication* **14**, 771–783.

Frey, F. A. (1984). Rare earth element abundances in upper mantle rocks. In: Henderson, P. (ed.) *Rare Earth Element Geochemistry*. Amsterdam: Elsevier, pp. 153–203.

Green, H. W., II & Gueguen, Y. (1974). Origin of kimberlite pipes by diapiric upwelling in the mantle. *Nature* **249**, 617–620.

Griffin, W. L., Smith, D., Boyd, F. R., Cousens, D. R., Ryan, C. G., Sie, S. H. & Suter, G. F. (1989). Trace element zoning in garnets from sheared mantle xenoliths. *Geochimica et Cosmochimica Acta* **53**, 561–567.

Griffin, W. L., O'Reilly, S. Y. & Ryan, C. G. (1999*a*). The composition and origin of subcontinental mantle lithosphere. In: Fei, Y., Bertka, C. M. & Mysen, B. O. (eds) *Mantle Petrology: Field Observations and High Pressure Experimentation: a Tribute to Francis R. (Joe) Boyd. Geochemical Society, Special Publication* **6**, 13–45.

Griffin, W. L., Shee, S. R., Ryan, C. G., Win, T. T. & Wyatt, B. A. (1999*b*). Harzburgite to lherzolite and back again: metasomatic processes in ultramafic xenoliths from the Wesselton kimberlite, Kimberley, South Africa. *Contributions to Mineralogy and Petrology* **134**, 232–250.

Grutzeck, M. W., Kridelbough, S. J. & Weill, D. F. (1974). The distribution of Sr and REE between diopside and the silicate liquid. *Geophysical Research Letters* **1**, 273–275.

Gurney, J. J. (1984). A correlation between garnets and diamonds. In: Glover, J. E. & Harris, P. G. (eds) *Kimberlite Occurrence and Origin: a Basis for Conceptual Models in Exploration. Geology Department and University Extension, University of Western Australia, Publication* **8**, 143–166.

Gurney, J. J. & Harte, B. (1980). Chemical variations in upper mantle nodules from southern African kimberlites. *Philosophical Transactions of the Royal Society of London, Series A* **297**, 273–293.

Gurney, J. J. & Switzer, G. S. (1973). The discovery of garnets closely related to diamonds in the Finsch pipe, South Africa. *Contributions to Mineralogy and Petrology* **39**, 103–116.

Gurney, J. J., Jacob, W. R. O. & Dawson, J. B. (1979). Megacrysts from the Monastery kimberlite pipe, South Africa. In: Boyd, F. R. & Meyer, H. O. A. (eds) *The Mantle Sample: Inclusions in Kimberlites and Other Volcanics*. Washington, DC: American Geophysical Union, pp. 227–243.

Hanson, G. N. (1980). Rare-earth elements in petrogenetic studies of igneous systems. *Annual Review of Earth and Planetary Sciences* **8**, 371–406.

Hart, S. R. & Dunn, T. (1993). Experimental cpx/melt partitioning of 24 trace elements. *Contributions to Mineralogy and Petrology* **113**, 1–8.

Harte, B. (1977). Rock nomenclature with particular relation to deformation and recrystallization textures in olivine-bearing xenoliths. *Journal of Geology*, **85**, 279–288.

Harte, B. (1978). Kimberlite nodules, upper mantle petrology and geotherms. *Philosophical Transactions of the Royal Society of London, Series A* **288**, 487–500.

Harte, B. (1983). Mantle peridotites and processes—the kimberlite sample. In: Hawkesworth, C. J. & Norry, M. J. (eds) *Continental Basalts and Mantle Xenoliths*. Nantwich: Shiva, pp. 46–91.

Harte, B. & Gurney, J. J. (1981). The mode of formation of chromium-poor megacryst suites from kimberlites. *Journal of Geology* **89**, 749–753.

Harte, B. & Hawkesworth, C. J. (1989). Mantle domains and mantle xenoliths. In: Ross, J., Jaques, A. L., Ferguson, J., Green, D. H., O'Reilly, S. Y., Danchin, R. V. & Janse, A. J. A. *Kimberlites and Related Rocks, Volume 2. Geological Society of Australia, Special Publication* **14**, 649–686.

Harte, B. & Kirkley, M. B. (1997). Partitioning of trace elements between clinopyroxene and garnet: data from mantle eclogites. *Chemical Geology*, **136**, 1–24.

Harte, B., Winterburn, P. A. & Gurney, J. J. (1987). Metasomatic phenomena in garnet peridotite facies mantle xenoliths from the Matsoku kimberlite pipe, Lesotho. In: Menzies, M. A. & Hawkesworth, C. J. (eds) *Mantle Metasomatism*. London: Academic Press, pp. 145–220.

Harte, B., Hunter, R. H. & Kinny, P. D. (1993). Melt geometry, movement and crystallization in relation to mantle dykes, veins and metasomatism. *Philosophical Transactions of the Royal Society of London, Series A* **342**, 1–21.

Harte, B., Fitzsimons, I. C. W. & Kinny, P. D. (1996). Clinopyroxene–garnet trace element partition coefficients for mantle peridotite and melt assemblages. V. M. Goldschmidt Conference, Heidelberg. *Journal of Conference Abstracts* **1**, 235.

Hinton, R. W. (1990). Ion microprobe trace element analysis of silicates: measurement of multi-element glasses. *Chemical Geology* **83**, 11–25.

Hoal, K. E. O., Hoal, B. G., Erlank, A. J. & Shimizu, N. (1994). Metasomatism of the mantle lithosphere recorded by rare earth elements in garnets. *Earth and Planetary Science Letters* **126**, 303–313.

Hops, J. J. (1989). Some aspects of the geochemistry of high-temperature peridotites and megacrysts from the Jagersfontein kimberlite pipe, South Africa. Ph.D. thesis, University of Cape Town.

Hops, J. J., Gurney, J. J., Harte, B. & Winterburn, P. A. (1989). Megacrysts and high temperature nodules from the Jagersfontein kimberlite pipe. In: Ross, J., Jaques, A. L., Ferguson, J., Green, D. H., O'Reilly, S. Y., Danchin, R. V. & Janse, A. J. A. *Kimberlites and Related Rocks, Vol 2. Geological Society of Australia, Special Publication* **14**, 759–770.

Hops, J. J., Gurney, J. J. & Harte, B. (1992). The Jagersfontein Cr-poor megacryst suite—towards a model for megacryst petrogenesis. In: Cox, K. G. & Baker, P. E. (eds) *Essays on Magmas and Other Earth Fluids. Journal of Volcanology and Geothermal Research* **50**, 143–160.

Ionov, D. A., Bodinier, J.-L., Musaka, S. B. & Zanetti, A. (2002). Mechanisms and sources of mantle metasomatism: major and trace element compositions of peridotite xenoliths from Spitsbergen in the context of numerical modelling. *Journal of Petrology* **43**, 2219–2259.

Ionov, D. A., Musaka, S. B. & Bodinier, J.-L. (2002). Sr–Nd–Pb isotopic compositions of peridotite xenoliths from Spitsbergen: numerical modelling indicates Sr–Nd decoupling in the mantle by melt percolation metasomatism. *Journal of Petrology* **43**, 2261–2278.

Jones, R. A. (1987). Strontium and neodymium isotopic and rare earth evidence for the genesis of megacrysts in kimberlites of southern Africa. In: Nixon, P. H. (ed.) *Mantle Xenoliths*. New York: John Wiley, pp. 711–724.

Kramers, J. D., Roddick, J. C. M. & Dawson, J. B. (1983). Trace element and isotopic studies on veined, metasomatic and 'MARID' xenoliths from Bultfontein, South Africa. *Earth and Planetary Science Letters* **65**, 90–106.

Lawless, P. J., Gurney, J. J. & Dawson, J. B. (1979). Polymict peridotites from the Bultfontein and De Beers mines, Kimberley, South Africa. In: Boyd, F. R. & Meyer, H. O. A. (eds) *The Mantle Sample: Inclusions in Kimberlites and Other Volcanics*. Washington, DC: American Geophysical Union, pp. 145–155.

Matthews, M., Harte, B. & Prior, D. (1992). Mantle garnets: a cracking yarn. *Geochimica et Cosmochimica Acta* **56**, 2633–2642.

McKenzie, D. P. (1984). The generation and compaction of partially molten rock. *Journal of Petrology* **25**, 713–765.

McKenzie, D. P. (1989). Some remarks on the movement of small melt fractions in the mantle. *Earth and Planetary Science Letters* **95**, 53–72.

McKenzie, D. & O'Nions, R. K. (1991). Partial melt distributions from inversion of rare earth element concentrations. *Journal of Petrology* **32**, 1021–1091.

Menzies, A. H., Carlson, R. W., Shirey, S. B. & Gurney, J. J. (1999). Re–Os systematics of Newlands peridotite xenoliths: implications for diamond and lithosphere formation. In: Gurney, J. J., Gurney, J. L., Pascoe, M. D. & Richardson, S. H. (eds) *Proceedings of the 7th Kimberlite Conference (Nixon Volume)*. Cape Town: Red Roof Design, pp. 566–573.

Menzies, M. A., Kempton, P. & Dungan, M. (1985). Interaction of the continental lithosphere and asthenospheric melts below the Geronimo Volcanic Field, Arizona, U.S.A. *Journal of Petrology* **26**, 663–693.

Menzies, M. A. & Hawkesworth, C. J. (eds) (1987). *Mantle Metasomatism*. London: Academic Press.

Mercier, J.-C. C. (1979). Peridotite xenoliths and the dynamics of kimberlite intrusion. In: Boyd, F. R. & Meyer, H. O. A. (eds) *The Mantle Sample: Inclusions in Kimberlites and Other Volcanics*. Washington, DC: American Geophysical Union, pp. 197–212.

Morfi, L. (2001). Polymict peridotites and mantle processes. Ph.D. thesis, University of Edinburgh.

Navon, O. & Stolper, E. (1987). Geochemical consequences of melt percolation: the upper mantle as a chromatographic column. *Journal of Geology* **95**, 285–307.

Nielson, J. E. & Wilshire, H. G. (1993). Magma transport and metasomatism in the mantle: a critical review of current geochemical models. *American Mineralogist* **78**, 1117–1134.

Nixon, P. H. & Boyd, F. R. (1973*a*). Petrogenesis of the granular and sheared ultrabasic nodule suite in kimberlites. In: Nixon, P. H. (ed.) *Lesotho Kimberlites*. Maseru: Lesotho National Development Corporation, pp. 48–56.

Nixon, P. H. & Boyd, F. R. (1973*b*). The discrete nodule association in kimberlites from northern Lesotho. In: Nixon, P. H. (ed.) *Lesotho Kimberlites*. Maseru: Lesotho National Development Corporation, pp. 67–75.

Nixon, P. H., van Calsteren, P. W. C., Boyd, F. R. & Hawkesworth, C. J. (1987). Harzburgites with garnets of diamond facies from southern African kimberlites. In: Nixon, P. H. (ed.) *Mantle Xenoliths*. Chichester: John Wiley, pp. 523–533.

Nowell, G. M., Pearson, D. G., Kempton, P. D., Noble, S. R. & Smith, C. B. (1999). Origins of kimberlites: a Hf isotope perspective. In: Gurney, J. J., Gurney, J. L., Pascoe, M. D. & Richardson, S. H. (eds) *Proceedings of the 7th Kimberlite Conference (Nixon Volume)*. Cape Town: Red Roof Design, pp. 616–624.

O'Neill, H. St. C. & Wood, B. J. (1979). An experimental study of Fe–Mg partitioning between garnet and olivine and its calibration as a geothermometer. *Contributions to Mineralogy and Petrology* **70**, 59–70.

Parmentier, E. M. & Turcotte, D. C. (1974). An explanation of the pyroxene geotherm based on plume convection in the mantle. *Earth and Planetary Science Letters* **24**, 209–212.

Pearson, D. G. & Shirey, R. B. (1999). Isotopic dating of diamonds. In: Ruiz, J. & Lambert, D. D. (eds) *Applications of Radiogenic Isotopes to Ore Deposit Research. SEG Reviews in Economic Geology* **9**, 143–171.

Pearson, D. G., Carlson, R. W., Shirey, S. B., Boyd, F. R. & Nixon, P. H. (1995*a*). The stabilization of Archaean lithospheric mantle: a Re–Os isotope study of peridotite xenoliths from the Kaapvaal craton. *Earth and Planetary Science Letters* **134**, 341–357.

Pearson, D. G., Shirey, S. B. Carlson, R. W., Boyd, F. R., Pokhilenko, N. P. & Shimizu, N. (1995*b*). Re–Os, Sm–Nd, Rb–Sr isotope evidence for thick Archaean lithospheric mantle beneath the Siberian craton modified by multi-stage metasomatism. *Geochimica et Cosmochimica Acta* **59**, 959–977.

Richardson, S. H. & Harris, J. W. (1997). Antiquity of peridotitic diamonds from the Siberian Craton. *Earth and Planetary Science Letters* **151**, 271–277.

Richardson, S. H., Gurney, J. J., Erlank, A. J. & Harris, J. W. (1984). Origin of diamonds in old enriched mantle. *Nature* **310**, 198–202.

Richardson, S. H., Erlank, A. J. & Hart, S. R. (1985). Kimberlite-borne garnet peridotite xenoliths from old enriched subcontinental lithosphere. *Earth and Planetary Science Letters* **75**, 116–128.

Schulze, D. J. (1995) Low-Ca garnet harzburgites from Kimberley, South Africa: abundance and bearing on structure and evolution of the lithosphere. *Journal of Geophysical Research* **100**, 12513–12519.

Shimizu N. (1975). Rare earth elements in garnets and clinopyroxenes from garnet lherzolite nodules in kimberlites. *Earth and Planetary Science Letters* **25**, 26–32.

Shimizu, N. (1999). Young geochemical features in cratonic peridotites from southern Africa and Siberia. In: Fei, Y., Bertka, C. M. & Mysen, B. O. (eds) *Mantle Petrology: Field Observations and High Pressure Experimentation: a Tribute to Francis R. (Joe) Boyd. Geochemical Society, Special Publication* **6**, 47–55.

Shimizu, N. & Kushiro, I. (1975) The partitioning of rare earth elements between garnet and liquid at high pressures: preliminary experiments. *Geophysical Research Letters* **3**, 413–416.

Shimizu, N. & Richardson, S. H. (1987). Trace element abundance patterns of garnet inclusions in peridotite-suite diamonds. *Geochimica et Cosmochimica Acta* **51**, 755–758.

Shimizu, N. & Sobolev, N. V. (1995). Young peridotitic diamonds from the Mir kimberlite pipe. *Nature* **375**, 394–397.

Shimizu, N., Sobolev, N. V. & Pokhilenko, N. P. (1994). Chemical zoning of garnets in peridotites and diamonds. *Mineralogical Magazine* **58A**, 831–832.

Shimizu, N., Sobolev, N. V. & Yefimova, E. S. (1997). Chemical heterogeneities of inclusion garnets and juvenile character of peridotitic diamonds from Siberia. *Russian Geology and Geophysics* **38**, 356–372.

Shimizu, N., Kopylova, M. G., Russell, J. K. & Cookenboo, H. (1999). Trace element characteristics of peridotitic xenoliths from the Jericho kimberlite pipe, north central Slave Craton, Canada. *Ofioliti* **24**, 165.

Smith, C. B. (1983). Pb, Sr and Nd isotopic evidence for sources of southern African Cretaceous kimberlites. *Nature* **304**, 51–54.

Smith, D. & Boyd, F. R. (1987). Compositional heterogeneities in a high-temperature lherzolite nodule and implications for mantle processes. In: Nixon, P. H. (ed.) *Mantle Xenoliths*. Chichester: John Wiley, pp. 551–561.

Smith, D. & Boyd, F. R. (1992). Compositional zonation in garnets in peridotite xenoliths. *Contributions to Mineralogy and Petrology* **112**, 134–147.

Smith, D. & Ehrenberg, S. N. (1984). Zoned minerals in garnet peridotite nodules from the Colorado Plateau: implications for mantle metaomatism and kinetics. *Contributions to Mineralogy and Petrology* **86**, 274–285.

Sobolev, N. V. (1977). *Deep-seated Inclusions in Kimberlites and the Problem of the Composition of the Upper Mantle*. Washington, DC: American Geophysical Union.

Sun, S. S. & McDonough, W. F. (1989). Chemical and isotopic systematics of ocean basalts; implications for mantle composition and processes. In: Saunders, E. D. & Norry, M. J. (eds) *Magmatism in the Ocean Basins. Geological Society, London, Special Publications* **42**, 313–345.

Tainton, K. M. & McKenzie, D. (1994). The generation of kimberlites, lamproites, and their source rocks. *Journal of Petrology* **35**, 787–817.

Van Westrenen, W., Blundy, J. & Wood, B. J. (1999). Crystal-chemical controls on trace element partitioning between garnet and anhydrous silicate melt. *American Mineralogist* **84**, 838–847.

Vernières, J., Godard, M. & Bodinier, J.-L. (1997). A plate model for the simulation of trace element fractionation during partial melting and magma transport in the Earth's upper mantle. *Journal of Geophysical Research* **102**, 24771–24784.

Wilshire, H. G. (1987). *A Model of Mantle Metasomatism. Geological Society of America, Special Volume* **215**, 47–60.

Winterburn, P. A. (1987). Geochemical studies of peridotite xenoliths from South African kimberlites. Ph.D. thesis, University of Edinburgh.

Winterburn, P. A., Harte, B. & Gurney, J. J. (1990). Peridotite xenoliths from the Jagersfontein kimberlite pipe: I. Primary and primary–metasomatic mineralogy. *Geochimica et Cosmochimica Acta* **54**, 329–341.

Witt-Eickschen, G. & Harte, B. (1994). Distribution of trace elements between amphibole and clinopyroxene from mantle peridotites of the Eifel (west Germany): an ion-microprobe study. *Chemical Geology* **117**, 235–250.

Wyllie, P. J. (1989). The genesis of kimberlites and some low-SiO_2, high alkali magmas. In: Ross, J., Jaques, A. L., Ferguson, J., Green, D. H., O'Reilly, S. Y., Danchin, R. V. & Janse, A. J. A. *Kimberlites and Related Rocks, Volume 1. Geological Society of Australia, Special Publication* **14**, 603–615.

Wyllie, P. J. & Ryabchikov, I. D. (2000). Volatile components, magmas, and critical fluids in upwelling mantle. *Journal of Petrology* **41**, 1195–1206.

Zinner, E. & Crozaz, G. (1986). Ion probe determination of the abundances of all the rare earth elements in single mineral grains. In: Benninghoven, A., Colton, R. J., Simons, D. S. & Werner, H. W. (eds) *Secondary Ion Mass Spectrometry SIMS V*. Berlin: Springer, pp. 444–447.